

# The Cosmic Microwave Background - Secondary Anisotropies

Federico Bianchini<sup>a,b,c</sup> and Abhishek Maniar<sup>a,b,c</sup>

<sup>a</sup>SLAC National Accelerator Laboratory, 2575 Sand Hill Road, Menlo Park, CA, 94025, USA

<sup>b</sup>Kavli Institute for Particle Astrophysics and Cosmology, Stanford University, 452 Lomita Mall, Stanford, CA, 94305, USA

<sup>c</sup>Department of Physics, Stanford University, 382 Via Pueblo Mall, Stanford, CA, 94305, USA

© 20xx Elsevier Ltd. All rights reserved.

Chapter Article tagline: update of previous edition., reprint..

## Nomenclature

CMB	Cosmic Microwave Background
LSS	Large Scale Structure
BAO	Baryonic Acoustic Oscillations
$\Lambda\text{CDM}$	Lambda Cold Dark Matter (the cosmological concordance model)
ISW	Integrated Sachs-Wolfe effect
RS	Rees-Sciama effect
ML	Moving Lens effect
(t/k)SZ	(Thermal/Kinematic) Sunyaev-Zel'dovich effect
ACT	Atacama Cosmology Telescope
SPT	South Pole Telescope
QE	Quadratic Estimator
$C_L^{\phi\phi}$	CMB lensing auto-spectrum
$y$	Comptonization parameter
$\tau$	Optical depth parameter

## Abstract

The cosmic microwave background (CMB), the relic radiation from the early Universe, offers a unique window into both primordial conditions and the intervening large-scale structure (LSS) it traverses. Interactions between CMB photons and the evolving Universe imprint secondary anisotropies—modifications to the CMB's intensity and polarization caused by gravitational effects and scattering processes. These anisotropies serve as a powerful probe of fundamental physics while also revealing astrophysical processes governing the thermodynamics and distribution of baryonic matter. In this chapter, we provide a comprehensive review of the physical mechanisms underlying secondary anisotropies, their observational status, and their potential to advance precision cosmology. With the increasing sensitivity of CMB experiments and synergy with LSS surveys, secondary anisotropies are poised to unveil unprecedented insights into the Universe's composition, evolution, and dynamics.

### Key Points

- The CMB provides a snapshot of the Universe at the time of recombination, while also acting as a backlight for the large-scale structure (LSS) it traverses.
- Secondary anisotropies arise from two main mechanisms: gravitational effects (e.g., lensing and the Integrated Sachs-Wolfe effect) and scattering processes (e.g., Sunyaev-Zel'dovich effects and patchy screening).
- Secondary anisotropies are powerful tools for mapping gravitational potentials, as well as the distribution and thermal state of gas across cosmic time.
- Current experiments like *Planck*, ACT, and SPT, along with next-generation surveys such as the Simons Observatory and CMB-S4, promise transformative insights into secondary anisotropies, particularly through synergies with LSS surveys.

## 1 Introduction

The cosmic microwave background (CMB) provides our earliest view of the Universe, offering a snapshot of its state at the time of recombination and decoupling, when neutral hydrogen atoms formed. Observations of the CMB from full-sky satellite missions, such as WMAP (Komatsu et al., 2009) in the 2000s and *Planck* (Planck Collaboration et al., 2020a) in the 2010s, have revolutionized cosmology, serving as a goldmine of information about the Universe's origins, composition, and evolution. These observations have played a pivotal role in establishing the concordance cosmological model, also known as the  $\Lambda\text{CDM}$  model. At the same time, high-resolution, low-noise ground-based experiments, such as the South Pole Telescope (SPT, Carlstrom et al., 2011; Sobrin et al., 2022) and the Atacama Cosmology Telescope (ACT, Swetz et al., 2011; Henderson et al., 2016), have extended our knowledge of the CMB by probing smaller angular scales and polarization with unprecedented sensitivity. Upcoming experiments, including the Simons Observatory (SO, Ade et al., 2019), and

Useful estimates		
$\theta_{\text{lens}} \sim 1', \int \dot{\Phi} d\eta \sim 10^{-4}, \frac{k_B T_e}{m_e c^2} \sim \left(\frac{v_{\text{th}}}{c}\right)^2 \approx 0.01, \frac{v_{\text{bulk,rot}}}{c} \sim 10^{-3}, \frac{\delta T_0}{T_0} \sim a_2 \sim 10^{-5}$		
Effect	$\delta T^{\text{effect}}/T_0 \propto$	Information
Gravitational secondaries		
Lensing	$\theta_{\text{lens}}$	Mapping the total matter, cosmological constraints
ISW, Rees-Sciama	$\int \dot{\Phi} d\eta$	Dark energy, curvature
Moving Lens	$v_{\text{bulk}} \perp$	Transverse velocity field
Scattering secondaries		
tSZ, relativistic tSZ	$\tau(v_{\text{th}}/c)^{2,4}$	Thermal pressure, temperature
kSZ, rotational kSZ	$\tau(v_{\text{bulk}} \parallel/c)$	Density, LOS velocity field
Polarized SZ	$\tau(v_{\text{bulk}} \perp/c)^2, \tau a_2$	Density, remote CMB quadrupole
Patchy screening	$\tau(\delta T_0/T_0)$	Density

Fig. 1: Summary of various secondary CMB anisotropies, highlighting their order-of-magnitude estimates and the types of information they provide about the Universe. The table distinguishes between gravitational and scattering secondaries, with key parameters such as typical lensing deflection angle ( $\theta_{\text{lens}}$ ), CMB temperature fluctuations ( $\delta T_0/T_0$ ), and velocity terms ( $v_{\text{th}}, v_{\text{bulk}}, v_{\text{rot}}$ ) used to describe their effects. Symbols  $\parallel$  and  $\perp$  denote components parallel and perpendicular to the line-of-sight, while  $a_2$  represents the CMB temperature quadrupole. Special thanks to Emmanuel Schaan for permission to reproduce this figure.

CMB-S4 ([Abazajian et al., 2022](#)) promise to further refine our understanding by pushing the boundaries of precision cosmology.

The CMB encodes the acoustic fluctuations imprinted in the primordial plasma, making it extremely sensitive to the Universe's initial conditions and composition (e.g., [Silk, 1967](#); [Sachs and Wolfe, 1967](#); [Peebles and Yu, 1970](#); [Doroshkevich et al., 1978](#)). However, this pristine snapshot does not tell the whole story. The CMB also acts as a backlight for the intervening large-scale structure (LSS), and its photons interact with cosmic structures on their journey to us. These interactions alter the frequency, energy, and direction of propagation of the CMB photons, generating what are known as secondary anisotropies. Secondary anisotropies are classified into two broad families based on their underlying physical mechanisms. The first family arises from gravitational effects, including weak gravitational lensing, decaying gravitational potentials (the integrated Sachs-Wolfe effect, or ISW), the Rees-Sciama effect (RS), and the moving lens (ML) effect. These anisotropies are sourced by the interaction of CMB photons with gravitational potential wells. The second family originates from scattering processes, such as inverse Compton scattering (the Sunyaev-Zel'dovich, or SZ effects) and Thomson scattering (e.g., patchy screening). These effects involve interactions between CMB photons and free electrons in the intervening cosmic gas.

Secondary anisotropies encode a wealth of information about both fundamental physics—such as the mass of neutrinos, and the properties of dark matter and dark energy—and astrophysics, including the thermodynamics of gas over cosmic time. By studying these effects, summarized in Fig. 1, we can extract insights into the composition and evolution of the Universe, as well as the processes shaping its structure. This chapter is devoted to reviewing the physical mechanisms behind these secondary anisotropies and their observational status, as well as highlighting the transformative potential of upcoming surveys. For additional reviews on the subject, see, e.g., [Hu and Dodelson \(2002\)](#); [Aghanim et al. \(2008\)](#).

## 2 Gravitational Secondaries

Gravitational secondary anisotropies arise from the interaction of CMB photons with intervening gravitational potentials along their path. These anisotropies have two primary sources: gravitational lensing and differential redshift caused by time-varying metric perturbations. To describe these effects, we begin with the line element  $ds^2$  of a perturbed, spatially flat Friedmann-Lemaître-Robertson-Walker (FLRW)

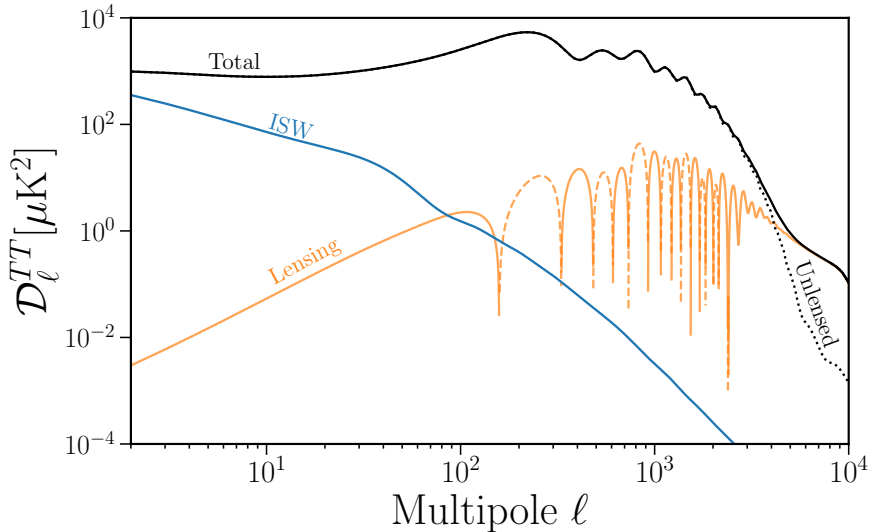


Fig. 2: Power spectra of secondary temperature anisotropies from gravitational effects, normalized as  $\mathcal{D}_\ell^{TT} \equiv \frac{\ell(\ell+1)}{2\pi} C_\ell^{TT}$ . The blue line represents the late-time Integrated Sachs-Wolfe (ISW) effect. The orange line shows the gravitational lensing contribution, calculated as the difference between the lensed (black solid line) and unlensed (black dotted line) CMB  $TT$  power spectra. The dashed orange line highlights the negative component of the lensing term.

metric. In the conformal Newtonian (or longitudinal) gauge, the metric takes the form (Ma and Bertschinger, 1995):

$$ds^2 = a^2(\eta) \left[ -(1 + 2\Psi_N) d\eta^2 + (1 + 2\Phi_N) \gamma_{ij} dx^i dx^j \right], \quad (1)$$

where  $a(\eta)$  is the scale factor depending on conformal time  $\eta$ ,  $\Phi_N$  and  $\Psi_N$  are the scalar metric potentials<sup>1</sup> (Bardeen, 1980), and  $\gamma_{ij}$  is the unperturbed spatial metric:

$$\gamma_{ij} dx^i dx^j = d\chi^2 + \chi^2 (d\theta^2 + \sin^2 \theta d\phi^2), \quad (2)$$

where  $\chi$  is the comoving radial distance. The metric in Eq. 1 resembles the weak-field limit of General Relativity near Minkowski space. In this limit,  $\Phi_N$  acts as the gravitational potential governing the dynamics of non-relativistic objects, while the Weyl potential, defined as  $\Psi_\gamma \equiv (\Psi_N - \Phi_N)/2$ , determines the propagation of light by describing null geodesics. In the absence of anisotropic stress—associated with the trace-free component of the stress-energy tensor  $T_{ij}$ —the scalar potentials satisfy  $\Psi_N = -\Phi_N$ . This approximation holds in standard cosmological models during the matter- and dark-energy-dominated epochs, where contributions from anisotropic stress are negligible. By adopting the perturbed FLRW metric in the conformal Newtonian gauge, we establish the framework for analyzing gravitational secondary anisotropies. This formalism underpins the study of effects such as gravitational weak lensing, the integrated Sachs-Wolfe (ISW) effect, the Rees-Sciama effect, and moving lens effects. The temperature power spectra of selected gravitational secondary anisotropies are illustrated in Fig. 2.

## 2.1 Gravitational weak lensing

After recombination at redshift  $z \sim 1090$ , CMB photons traverse an evolving and clumpy universe before reaching our telescopes. Along the way, their trajectories are deflected by the gravitational potentials of LSS (Blanchard and Schneider, 1987). These deflections, typically on the order of 2 arcminutes and coherent over degree scales, leave distinct imprints on the observed CMB: they blur the sharp acoustic peaks (Seljak, 1996), transfer power from large to small scales (Metcalf and Silk, 1997), induce non-Gaussian features in the anisotropies (Bernardeau, 1997; Zaldarriaga, 2000), and convert a fraction of  $E$ -mode polarization into  $B$ -modes (Zaldarriaga and Seljak, 1998). CMB lensing serves a dual role in cosmology. On the one hand, it provides a valuable probe of the integrated gravitational potentials along the line-of-sight, offering insights into the distribution of matter and the growth of cosmic structures (e.g., Stompor and Efstathiou, 1999; Acquaviva and Baccigalupi, 2006). On the other hand, it acts as an obstacle by obscuring our view of primordial fluctuations, complicating the measurement of the tensor-to-scalar ratio parameter  $r$  (Knox and Song, 2002). The CMB is particularly advantageous for lensing studies due to its unique properties. As a single, well-defined source plane at  $z \sim 1090$ , the CMB lies behind all structure in the observable Universe. This unique position allows it to probe the LSS over the entire sky, complementing galaxy lensing observations, which typically focus on lower redshifts. Unlike galaxy surveys, the precisely known redshift of the CMB eliminates uncertainties related to source distances. Additionally, the intrinsic fluctuations in the CMB are predominantly Gaussian, simplifying the lensing reconstruction process. CMB

<sup>1</sup>Here, we consider only scalar perturbations.

## 4 The Cosmic Microwave Background - Secondary Anisotropies

lensing primarily originates from linear and mildly non-linear scales, which makes them easier to model and interpret compared to galaxy lensing, where contributions from highly non-linear scales are significant (e.g., [Amon and Efstathiou, 2022](#)). These properties make CMB lensing a powerful cosmological tool, enabling precise mapping of the matter distribution, constraints on key cosmological parameters, and investigations into the nature of dark energy and dark matter. For comprehensive reviews of CMB lensing, we refer the reader to [Lewis and Challinor \(2006\)](#); [Hanson et al. \(2010\)](#).

The lensing effect on CMB anisotropies can be described as a remapping of the unlensed CMB anisotropies,  $\tilde{X}(\hat{\mathbf{n}})$ , by the deflection angle  $\mathbf{d}(\hat{\mathbf{n}})$  (e.g., [Lewis and Challinor, 2006](#)):<sup>2</sup>

$$X(\hat{\mathbf{n}}) = \tilde{X}[\hat{\mathbf{n}} + \mathbf{d}(\hat{\mathbf{n}})], \quad (3)$$

where  $X(\hat{\mathbf{n}})$  represents the observed temperature  $T(\hat{\mathbf{n}})$  or polarization  $P_{\pm}(\hat{\mathbf{n}}) = [Q \pm iU](\hat{\mathbf{n}})$  anisotropies. Lensing preserves the blackbody spectrum and surface brightness of the CMB by altering the angle and magnification of the source without changing the photon frequency or density per unit solid angle. The deflection field  $\mathbf{d}(\hat{\mathbf{n}})$  in Eq. 3 can be decomposed into gradient and curl components (e.g., [Hirata and Seljak, 2003](#)):

$$\mathbf{d}(\hat{\mathbf{n}}) = \nabla\phi(\hat{\mathbf{n}}) + (\star\nabla)\omega(\hat{\mathbf{n}}), \quad (4)$$

where  $\phi(\hat{\mathbf{n}})$  is the scalar lensing potential,  $\omega(\hat{\mathbf{n}})$  is the curl component (or “pseudo-scalar lensing potential”), and  $\star\nabla$  denotes the derivative with a 90° counterclockwise rotation in the plane perpendicular to the line-of-sight ([Namikawa et al., 2012](#)).

The scalar lensing potential,  $\phi(\hat{\mathbf{n}})$ , is given by a line-of-sight integral:

$$\phi(\hat{\mathbf{n}}) = -2 \int_0^{\chi_*} d\chi \left( \frac{\chi_* - \chi}{\chi_* \chi} \right) \Psi_\gamma(\chi \hat{\mathbf{n}}, \eta_0 - \chi), \quad (5)$$

where  $\eta_0 - \chi$  is the conformal time when the photon was at location  $\chi \hat{\mathbf{n}}$ ,  $\Psi_\gamma$  is the Weyl potential (see Sec. 2), and the integral is evaluated along the unperturbed photon path under the Born approximation (e.g., [Hirata and Seljak, 2003](#)). The lensing convergence,  $\kappa(\hat{\mathbf{n}})$ , quantifies the local magnification effect on CMB anisotropies and is defined as the two-dimensional Laplacian of the lensing potential:  $\kappa(\hat{\mathbf{n}}) = -\frac{1}{2}\nabla^2\phi(\hat{\mathbf{n}})$ . Using the cosmological Poisson equation,  $\nabla^2\Phi \propto \delta_m$ ,<sup>3</sup> the lensing convergence can be related to the projected matter distribution  $\delta_m$  along the line-of-sight:

$$\kappa(\hat{\mathbf{n}}) = \int d\chi W^\kappa(\chi) \delta_m(\chi \hat{\mathbf{n}}, \eta_0 - \chi), \quad (6)$$

where the lensing kernel  $W^\kappa(\chi)$  describes the lensing efficiency, peaking around  $z \approx 2$ . At linear order, scalar metric perturbations, such as matter density fluctuations, produce only the gradient mode  $\nabla\phi(\hat{\mathbf{n}})$ , while the curl mode is generally negligible and is often used as a systematic check in lensing analyses (e.g., [Cooray et al., 2005](#)). However, curl modes can arise from vector and tensor perturbations (e.g., [Li and Cooray, 2006](#); [Namikawa et al., 2012](#)) or higher-order effects beyond the Born approximation (e.g., [Pratten and Lewis, 2016](#); [Robertson and Lewis, 2024](#)). The Born approximation, extensively tested in simulations (e.g., [Calabrese et al., 2015](#); [Beck et al., 2018](#); [Fabbian et al., 2018](#)), introduces only minor corrections. Post-Born corrections to the convergence power spectrum are small, at approximately 0.2% ([Krause and Hirata, 2010](#); [Pratten and Lewis, 2016](#)), and their effects on CMB temperature and polarization anisotropies have been studied in detail ([Hagstotz et al., 2015](#); [Marozzi et al., 2016](#); [Pratten and Lewis, 2016](#)).

To estimate the typical scale of the lensing effect, consider a gravitational potential depth of  $|\Phi| \sim 2 \times 10^{-5}$ . This corresponds to deflection angles of  $|\mathbf{d}| \sim 10^{-4}$  radians and structure sizes of approximately 300 Mpc, as set by the scale of the peak of the matter power spectrum. A photon traveling from the last-scattering surface, roughly 14,000 Mpc away, encounters about  $14000/300 \sim 50$  independent deflections. The cumulative root-mean-square (rms) deflection is therefore  $\sqrt{50} \times 10^{-4} \sim 2$  arcminutes. The coherence scale of the deflection field is determined by the angular size of a typical 300 Mpc structure. At a comoving distance of  $\chi = 7000$  Mpc (halfway to the last-scattering surface), this corresponds to an angular scale of approximately  $300/7000 \sim 2$  degrees.

Lensing modifies the statistical properties of the observed CMB anisotropies. To gain intuition into its effects, we can Taylor-expand the remapping equation (Eq. 3):<sup>4</sup>

$$X(\hat{\mathbf{n}}) = \tilde{X}(\hat{\mathbf{n}}) + [\nabla\phi(\hat{\mathbf{n}}) + (\star\nabla)\omega(\hat{\mathbf{n}})] \cdot \nabla\tilde{X} + O(\phi^2, \omega^2), \quad (7)$$

where the additional terms are proportional to the gradients of the unlensed CMB fields. In the small-angle approximation, focusing on the temperature field and considering only the scalar potential, the first-order expansion in harmonic space becomes ([Hu, 2000](#)):

$$T_\ell \approx \tilde{T}_\ell - \int \frac{d^2 L}{2\pi} [\mathbf{L} \cdot (\boldsymbol{\ell} - \mathbf{L})] \phi_{\ell-L} \tilde{T}_L. \quad (8)$$

<sup>2</sup>Although not an exact remapping, this approximation is sufficiently accurate for most applications ([Lewis et al., 2017](#)).

<sup>3</sup>This assumes General Relativity and neglects minor effects from massive neutrinos.

<sup>4</sup>This expansion is not accurate on all scales, especially for lensing at scales comparable to the deflection angles. See [Challinor and Lewis \(2005\)](#) for an exact treatment.

Assuming that both  $\tilde{T}_\ell$  and  $\phi_\ell$  are isotropic Gaussian random fields and uncorrelated,<sup>5</sup> the lensed temperature power spectrum is given by:

$$C_\ell^{TT} \approx \left(1 - \ell^2 \int \frac{d \ln L}{4\pi} L^4 C_L^{\phi\phi}\right) C_\ell^{\tilde{T}\tilde{T}} + \int \frac{d^2 \mathbf{L}}{2\pi} [\mathbf{L} \cdot (\boldsymbol{\ell} - \mathbf{L})]^2 C_{|\boldsymbol{\ell}-\mathbf{L}|}^{\phi\phi} C_L^{\tilde{T}\tilde{T}}, \quad (9)$$

This equation shows that the lensed power spectrum is a convolution of the unlensed temperature gradient power spectrum  $C_L^{\tilde{T}\tilde{T}}$  with the deflection power spectrum  $C_L^{\phi\phi}$ . As shown by the oscillations and the asymptotic positive offset in the orange line of Fig. 2, lensing smooths the acoustic peaks in the CMB temperature anisotropies and enhances the small-scale power in the damping tail. Despite reshuffling power across scales, lensing conserves the total temperature variance since it preserves brightness while altering photon directions. Lensing has similar effects on  $C_\ell^{EE}$  and  $C_\ell^{TE}$  as it does on temperature anisotropies. Additionally, lensing converts a fraction of  $E$ -mode power into  $B$ -modes, creating a lensed  $C_\ell^{BB}$  signal (e.g. Zaldarriaga and Seljak, 1998). This leakage corresponds to an effective white-noise level of  $\sim 5\mu\text{K-arcmin}$  at  $\ell \lesssim 100$ , posing a significant contamination to searches for primordial gravitational waves using  $B$ -modes on large angular scales.

Lensing also introduces mode coupling, correlating previously independent harmonic modes  $\boldsymbol{\ell} \neq \boldsymbol{\ell}'$ , as shown in Eq. 8. For a fixed realization of the lenses, the CMB covariance matrix acquires off-diagonal elements:

$$\langle X_\ell Y_{\boldsymbol{\ell}-\mathbf{L}}^* \rangle_{\text{CMB}} = f_{\boldsymbol{\ell},\mathbf{L}}^{XY} \phi_L + O(\phi^2), \quad (\mathbf{L} \neq 0) \quad (10)$$

where  $\langle \cdot \rangle_{\text{CMB}}$  denotes an average over CMB realizations, and  $f_{\boldsymbol{\ell},\mathbf{L}}^{XY}$  are coupling kernels that depend on the observable  $X, Y \in [T, E, B]$ . These mode couplings provide the foundation for constructing quadratic estimators (QEs) of the lensing potential:

$$\hat{\phi}_L^{XY} = A_L^{XY} \int \frac{d\ell^2}{2\pi} F_{\boldsymbol{\ell},\mathbf{L}}^{XY} X_L Y_{\boldsymbol{\ell}-\mathbf{L}}, \quad (11)$$

where  $A_L^{XY}$  normalizes the estimator to ensure unbiasedness, and  $F_{\boldsymbol{\ell},\mathbf{L}}^{XY}$  is a filter optimized for maximal signal-to-noise ratio. For full expressions, see Hu and Okamoto (e.g., 2002); Maniyar et al. (e.g., 2021), and for the “shear-only” QE, see Schaan and Ferraro (2019). Beyond QEs, Bayesian methods leveraging the full CMB posterior have been proposed to extract higher-order information and approach optimality (e.g., Hirata and Seljak, 2003; Carron and Lewis, 2017; Millea et al., 2020; Millea and Seljak, 2022).

Once the lensing potential map is reconstructed, the lensing power spectrum can be calculated by subtracting noise bias terms (e.g., Hanson et al., 2011; Shen et al., 2024). The resulting spectrum is then compared with theoretical predictions to infer cosmological constraints. Within the base  $\Lambda\text{CDM}$  model, CMB lensing constrains a narrow elongated tube in the 3D subspace spanned by  $\sigma_8$ - $H_0$ - $\Omega_m$ , with the strongest constraint on the combination  $\sigma_8 \Omega_m^{0.25}$ . Combining CMB lensing with low-redshift galaxy BAO measurements breaks degeneracies among  $\sigma_8$ ,  $H_0$ , and  $\Omega_m$ , sharpening constraints on individual parameters.<sup>6</sup>

Since its first detection in 2007 by cross-correlating lensing maps from the Wilkinson Microwave Anisotropy Probe (WMAP) with NRAO VLA Sky Survey radio galaxies (Smith et al., 2007), CMB lensing science has advanced significantly. The *Planck* team reconstructed an almost full-sky lensing map and measured the lensing power spectrum with a significance of  $25\sigma$  using temperature data (Planck Collaboration et al., 2014a). More recently, high-significance measurements of the CMB lensing auto-spectrum have been achieved by ACT (Das et al., 2011; Sherwin et al., 2017; Qu et al., 2023), SPT (van Engelen et al., 2012; Story et al., 2015; Omori et al., 2017; Wu et al., 2019; Pan et al., 2023; Ge et al., 2024), and *Planck* (Planck Collaboration et al., 2014a, 2016a; Carron et al., 2022), with detection significances up to around  $40\sigma$ . A compilation of these measurements is shown in Fig. 3.

Cross-correlations between CMB lensing and other tracers of structure allow for the extraction of redshift-localized information about the growth rate of structure in the Universe—a technique often referred to as “CMB lensing tomography.” These correlations also provide valuable insights into astrophysical processes and offer greater control over systematic uncertainties (e.g., Schaan et al., 2017). CMB lensing maps have been cross-correlated with various tracers, including galaxy catalogs (e.g., Sherwin et al., 2012; Bianchini et al., 2015; Peacock and Bilicki, 2018; Bianchini and Reichardt, 2018; Omori et al., 2019; Marques and Bernui, 2020; Krolewski et al., 2020; Darwish et al., 2020; Alonso et al., 2023), galaxy lensing (e.g., Hand et al., 2015; Liu and Hill, 2015; Singh et al., 2017; Namikawa et al., 2019; Robertson et al., 2021), cosmic infrared background (CIB) fluctuations (e.g., Holder et al., 2013; Planck Collaboration et al., 2014b; van Engelen et al., 2015), thermal Sunyaev-Zel'dovich Compton- $y$  maps (e.g., Hill and Spergel, 2014; McCarthy and Hill, 2024), peculiar velocity catalogs (e.g., Giani et al., 2023), and radio background maps (e.g., Todarello et al., 2024). The complementarity of these probes, combined with their potential to break parameter degeneracies, has driven interest in joint analyses of auto- and cross-correlation spectra between multiple cosmic fields—a strategy commonly referred to as “ $N \times 2$  analyses” (e.g., Nicola et al., 2016; Abbott et al., 2019; Chang et al., 2023; Fang et al., 2024; Sgier et al., 2021).

Finally, an exciting possibility that has emerged in recent years is to use CMB lensing to measure the mass of samples of galaxies and galaxy clusters (e.g. Baxter et al., 2015; Madhavacheril et al., 2015; Geach and Peacock, 2017; Raghunathan et al., 2018, 2019a,b; Ansarinejad et al., 2024). This is an especially promising technique to measure the mass and calibrate the mass-observable scaling relations of clusters at  $z \gtrsim 1$ , where the rate of lensed background galaxies observed with high S/N drops significantly.

<sup>5</sup>Correlations such as  $\langle T\phi \rangle$  induced by secondary anisotropies (e.g., the ISW and SZ effects) are neglected. See Sec. 2.2 and Sec. 3.1.

<sup>6</sup>See Pan et al. (2014); Planck Collaboration et al. (2016a); Madhavacheril et al. (2023) for detailed discussions on parameter dependencies of the CMB lensing power spectrum.

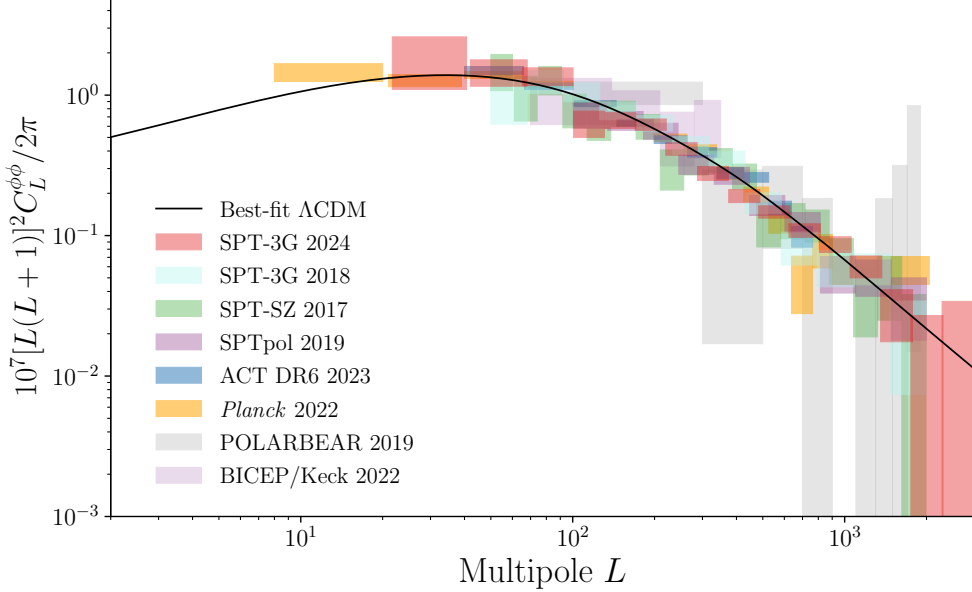


Fig. 3: Compilation of CMB lensing power spectrum measurements from various ground- and space-based CMB surveys. The solid black line corresponds to the best-fit  $\Lambda$ CDM model to the 2018 *Planck* TT, TE, EE+lowE+lensing dataset (Planck Collaboration et al., 2020a).

## 2.2 Integrated Sachs-Wolfe & Rees-Sciama effects

The Integrated Sachs-Wolfe (ISW) effect is a gravitational contribution to the observed CMB temperature fluctuations, arising from the time evolution of gravitational potentials as photons travel from the surface of last scattering to us. Depending on the regime and the underlying physical mechanism driving the potential evolution, this effect is sometimes referred to as the Rees-Sciama (RS) effect.

By solving the geodesic equation, photons traversing a time-varying gravitational potential  $\Phi_N$  experience an energy change, expressed in terms of temperature fluctuations as (e.g., Sach's and Wolfe, 1967).<sup>7</sup>

$$\frac{\Delta T_{\text{ISW}}(\hat{\mathbf{n}})}{T_{\text{CMB}}} = 2 \int_{\eta_0}^{\eta_*} d\eta e^{-\tau(\eta)} \dot{\Phi}_N(\hat{\mathbf{n}}, \eta), \quad (12)$$

where  $\tau(\eta)$  is the optical depth, and the dot denotes differentiation with respect to conformal time  $\eta$ . This temperature shift represents the redshifting or blueshifting of photons climbing out of a potential well that has changed since they entered it.

The late-time ISW effect arises from the decay of gravitational potentials at low redshifts, driven by the accelerated expansion of the universe due to dark energy. The gravitational potential  $\Phi_N$  can be related to the matter density fluctuations  $\delta_m$  via the Poisson equation. In Fourier space, under the Newtonian limit for subhorizon scales ( $k \gg aH$ ), this relation is:

$$\Phi_N(\mathbf{k}, \eta) = \frac{3}{2} \frac{\Omega_m}{a} \left( \frac{H_0}{k} \right)^2 \delta_m(\mathbf{k}, \eta). \quad (13)$$

During matter domination,  $\delta_m \propto a$ , leading to  $\dot{\Phi}_N \simeq 0$  and a negligible ISW effect. However, at lower redshifts, when dark energy dominates,  $\delta_m$  grows more slowly than  $a$ , causing  $\Phi_N$  to decay and  $\dot{\Phi}_N \neq 0$ . The ISW effect is achromatic (frequency-independent) and primarily contributes to large angular scales (low  $\ell$ ) in the CMB temperature power spectrum, as shown by the blue line in Fig. 2.

The strength of the ISW effect depends on the properties of dark energy (e.g., its equation of state and clustering), curvature, and potential modifications to gravity. However, the ISW signal is inherently weak and limited by cosmic variance. Crittenden and Turok (1996) proposed isolating the ISW effect through cross-correlation between CMB temperature maps and large-scale structure (LSS) tracers, as both probe the same gravitational potentials. The first detection of the ISW was achieved by cross-correlating WMAP first-year data with radio galaxy counts from NVSS and X-ray sources from HEAO1 A1 (Boughn and Crittenden, 2004). Subsequent analyses with various LSS tracers have yielded ISW detections with significances up to  $\sim 4\sigma$ , though some results remain inconclusive due to foreground contamination and differences in statistical methodologies (e.g., Fosalba et al., 2003; Giannantonio et al., 2006; Granett et al., 2008; Ferraro et al., 2015; Ade et al., 2016; Krolewski and Ferraro, 2022). Cosmic voids have also been used as tracers of gravitational potentials for ISW studies (e.g., Ilić et al., 2013; Kovács et al., 2019).

On smaller scales, the RS effect becomes significant, arising from non-linear gravitational collapse. If the photon crossing time through a structure is comparable to the potential evolution timescale, the net energy shift from the red- and blueshifting processes is nonzero,

<sup>7</sup>Assuming negligible anisotropic stress, such that  $\Phi_N = -\Psi_N$ .

leaving an imprint on the CMB. Originally described by [Rees and Sciama \(1968\)](#), the RS effect dominates the ISW effect at angular scales corresponding to  $\ell > 200$ . Unlike the ISW effect, the RS effect does not require dark energy, as non-linear gravitational collapse causes  $\delta_m$  to grow faster than  $a$ , leading to  $\dot{\Phi}_N < 0$  ([Cooray, 2002](#)). At late times, linear scales typically exhibit  $\dot{\Phi}_N > 0$ , while non-linear scales exhibit  $\dot{\Phi}_N < 0$ , resulting in opposite correlations between tracers and the CMB ([Nishizawa et al., 2008](#)).

The RS effect is currently too small to be detected by existing experiments. However, futuristic CMB experiments such as CMB-S4 or CMB-HD, in combination with Rubin LSST galaxies, may achieve modest detections with signal-to-noise ratios of  $S/N \sim 6 - 8$  ([Ferraro et al., 2022](#)). For a detailed review of the ISW and RS effects, we refer the reader to [Nishizawa \(2014\)](#).

### 2.3 Moving lens effect

The moving lens (ML) effect, also known as the "slingshot effect" (e.g., [Birkinshaw and Gull, 1983](#); [Tului and Laguna, 1995](#); [Stebbins, 2006](#)), is deeply related to the Rees-Sciama (RS) effect and arises from the transverse motion of gravitational potentials across the observer's line-of-sight. This motion generates a dipole signal in the CMB, aligned with the direction of motion. Specifically, CMB photons entering ahead of a moving structure (e.g., a galaxy cluster or supercluster) are redshifted, while those in the structure's wake are blueshifted. The resulting dipolar imprint is proportional to the transverse velocity  $v_\perp$  and the depth of the potential well, which scales with the total mass  $M_{\text{tot}}$  of the halo.

For a gravitational potential moving with a peculiar (comoving) velocity  $v_\perp$  transverse to the line-of-sight direction  $\hat{n}$ , the induced CMB temperature fluctuations are given by:

$$\frac{\Delta T_{\text{ML}}(\hat{n})}{T_{\text{ML}}} = -2 \int d\chi v_\perp \cdot \nabla_\perp \Phi_N(\chi \hat{n}), \quad (14)$$

where  $\nabla_\perp \Phi_N$  is the gradient on the 2-sphere of the gravitational potential. Like the ISW and lensing effects, the ML effect has a blackbody frequency dependence and cannot be isolated through multi-frequency observations.

The amplitude of the ML signal is small and subdominant compared to other signals and residual foregrounds, making its detection challenging. Consequently, the ML effect is more likely to be detected statistically across an ensemble of objects rather than for individual halos. Recent years have seen renewed interest in this effect, with the development of novel estimators, including pairwise transverse-velocity estimators, oriented stacking techniques, and quadratic estimators (QEs), to evaluate its detectability with upcoming surveys ([Yasini et al., 2019](#); [Hotinli et al., 2019, 2021](#)). For instance, [Hotinli and Pierpaoli \(2024\)](#) suggest that next-generation Stage-4 CMB and LSS surveys could detect the ML effect with a significance of  $10 - 20\sigma$ . However, ongoing Stage-3 surveys, such as DESI and SO, are expected to achieve lower detection significance due to the smaller number of observed halos.

## 3 Scattering secondaries

Scattering secondary anisotropies arise from interactions between CMB photons and free electrons in the ionized medium, altering the energy, direction, or polarization of photons. These anisotropies are primarily sourced by two processes: inverse Compton scattering, which leads to the thermal and kinematic Sunyaev-Zel'dovich (SZ) effects, and Thomson scattering, which produces anisotropies associated with patchy screening. Scattering-induced effects provide insights into the thermodynamic state and distribution of baryonic matter, as well as the history of reionization and the evolution of cosmic structures. In Fig. 4, we illustrate the contributions of the SZ effects and patchy screening to the CMB temperature power spectrum.

### 3.1 Sunyaev-Zel'dovich (SZ) effects

One of the best-known and most extensively studied secondary anisotropies in the CMB is the SZ effect ([Sunyaev and Zeldovich, 1970, 1972](#)). The SZ effect originates from the inverse Compton scattering between CMB photons and free electrons in a hot, ionized gas along the line-of-sight, typically found in galaxy clusters (see Fig. 5). The SZ effect is broadly classified into two components: the thermal SZ (tSZ) effect and the kinematic SZ (kSZ) effect. The tSZ effect arises from the scattering of CMB photons by the random thermal motions of electrons in the hot gas, resulting in a distinctive spectral distortion of the CMB. In contrast, the kSZ effect is caused by the bulk motion of electrons relative to the CMB rest frame, leading to a Doppler shift of the CMB photons without altering their overall Planckian spectrum. These two effects can be considered as first- and second-order terms in the scattering of photons with a Planck distribution by moving electrons. The kSZ effect, being a first-order process, shifts the CMB spectrum without distorting its blackbody nature, whereas the tSZ effect, as a second-order process, induces spectral distortions. Typically, the thermal velocities of electrons within clusters are much larger than their bulk velocities, causing the tSZ effect to dominate. For typical cluster masses and velocities, the amplitude of the kSZ effect is approximately an order of magnitude smaller than that of the tSZ effect. For detailed reviews, see [Birkinshaw \(1999\)](#) and [Carlstrom et al. \(2002\)](#).

#### 3.1.1 Thermal SZ

The tSZ effect arises from the inverse Compton scattering of CMB photons by high-energy electrons in the hot intracluster medium of galaxy clusters. As CMB photons traverse this ionized gas, interactions with electrons at temperatures of  $10^7$  to  $10^8$  K upscatter the photons to higher energies. This process imprints a characteristic spectral distortion on the CMB, providing a powerful tool for studying galaxy clusters and the large-scale structure of the Universe.

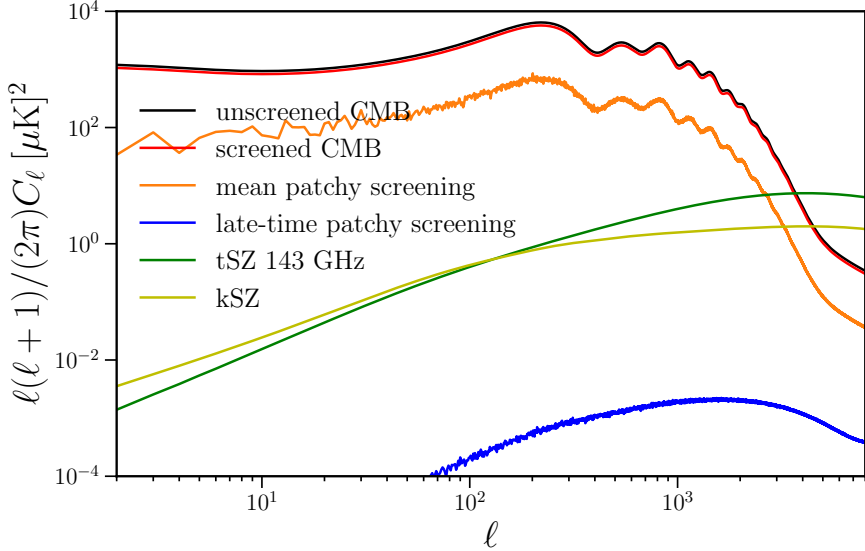


Fig. 4: Power spectra of secondary temperature anisotropies from scattering effects. The green and yellow lines represent the tSZ and kSZ effects respectively. The tSZ curve has been calculated assuming bandpass filters from the *Planck* experiment at 143 GHz. The orange line shows the mean patchy screening effect on the CMB power spectrum and the red curve is the resulting CMB power spectrum, calculated as the difference between the lensed (black solid line) CMB  $TT$  power spectra and orange curve. The blue curve presents the contribution of the “late-time” patchy screening ( $z < 5$ ) calculated using a template from AGORA simulations (Omori, 2024).

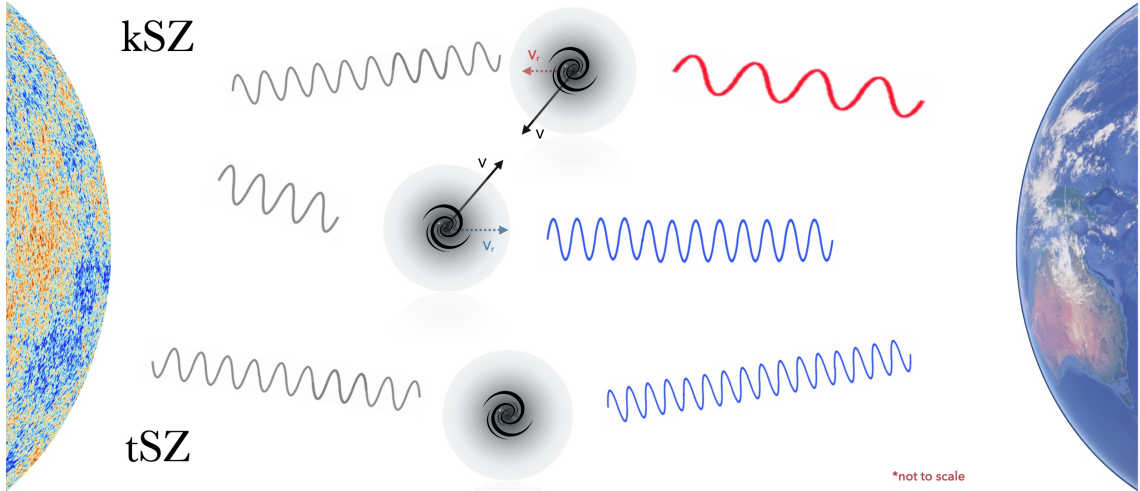


Fig. 5: Illustration of the thermal Sunyaev-Zel'dovich (tSZ) and kinematic Sunyaev-Zel'dovich (kSZ) effects. The tSZ effect (bottom) occurs when CMB photons are scattered by hot electrons in galaxy clusters, leading to a frequency-dependent distortion in the CMB spectrum (blue-shifted photons). The kSZ effect (top) arises due to the bulk motion of galaxy clusters relative to the CMB rest frame, introducing a Doppler shift in the scattered CMB photons. The colors represent shifts in photon frequencies, with red indicating a positive radial velocity (receding cluster) and blue a negative radial velocity (approaching cluster) relative to the observer.

The change in temperature/intensity of the CMB due to the tSZ effect can be described by the dimensionless Compton  $y$ -parameter, which quantifies the magnitude of the effect along a line-of-sight through the cluster. This change in temperature  $\Delta T_{\text{tSZ}}$  in the CMB is given by:

$$\frac{\Delta T_{\text{tSZ}}}{T_{\text{CMB}}} = f(x)y, \quad (15)$$

where  $f(x)$  accounts for the frequency dependence of the tSZ, and the  $y$ -parameter is given by:

$$y = \int \frac{k_B T_e}{m_e c^2} n_e \sigma_T \, dl, \quad (16)$$

where  $k_B$  is the Boltzmann constant,  $T_e$  is the electron temperature,  $m_e$  is the electron mass,  $c$  is the speed of light,  $n_e$  is the electron number density,  $\sigma_T$  is the Thomson cross-section,  $dl$  is the differential path length along the line-of-sight. This parameter essentially measures the integrated pressure of the electrons along the line-of-sight, making the tSZ effect sensitive to the electron distribution and thermal energy within the cluster. The frequency dependence of the tSZ  $f(x)$  is given as

$$f(x) = \left( x \frac{e^x + 1}{e^x - 1} - 4 \right), \quad (17)$$

where  $x = \frac{hv}{k_B T_{\text{CMB}}}$ . In general, observations in millimeter range are expressed in terms of specific intensity. For this purpose, the spectral distortion induced by the tSZ effect can be quantified by the change in the CMB intensity  $\Delta I_{\text{tSZ}}$ , which depends on the frequency  $\nu$  of the CMB photon. This change in intensity is described by:

$$\Delta I_{\text{tSZ}}(\nu) = y I_0 g(x), \quad (18)$$

where  $I_0 = \frac{2(k_B T_{\text{CMB}})^3}{(hc)^2}$  is the overall intensity scale, and the frequency dependence is given as

$$g(x) = \frac{x^4 e^x}{(e^x - 1)^2} \left( x \frac{e^x + 1}{e^x - 1} - 4 \right). \quad (19)$$

This frequency dependence produces a distinctive signature: at low frequencies (below 217 GHz), the tSZ effect manifests as a decrease in intensity, while at high frequencies (above 217 GHz), it appears as an increase in intensity. At approximately 217 GHz, the effect is null, as the energy gain and loss in the photon population cancel out, marking this as the crossover point (see Fig. 6). This characteristic frequency dependence enables a separation of the tSZ effect from other background radiation sources, such as synchrotron and dust emission.

The unique properties of the tSZ effect make it an invaluable tool for cosmology. As highlighted in Eq. 15 and 16, the temperature shift induced by the tSZ is proportional to the integrated pressure along the line of sight, making it unaffected by the inverse-square law that diminishes optical or X-ray brightness with distance. This independence from redshift enables the detection of distant and faint galaxy clusters, providing a powerful means to map the LSS. By analyzing the amplitude and spatial distribution of the  $y$ -parameter across numerous clusters, we can infer their mass distributions and investigate the thermal history of the universe, as well as energy feedback processes—such as those driven by active galactic nuclei (AGN)—that heat and redistribute gas within and around clusters.

The advent of arcminute-scale resolution experiments such as SPT, ACT, and *Planck* has transformed galaxy cluster science by enabling the identification of approximately mass-limited samples of massive galaxy clusters via the tSZ effect (e.g., Staniszewski et al., 2009; Menanteau et al., 2010; Reichardt et al., 2013; Hasselfield et al., 2013; Planck Collaboration et al., 2016c; Bleem et al., 2015; Huang et al., 2020; Hilton et al., 2021; Bleem et al., 2020). These tSZ-selected cluster catalogs have been instrumental in placing stringent constraints on cosmological models (e.g., Planck Collaboration et al., 2016b; Salvati et al., 2018; Zubeldia and Challinor, 2019; Bocquet et al., 2019). In addition, high-resolution, multi-frequency observations of the microwave sky have enabled the extraction of the thermal SZ Compton- $y$  parameter over vast regions using advanced component-separation algorithms (e.g., Planck Collaboration et al., 2016d; Madhavacheril et al., 2019; Bleem et al., 2022; Coulton et al., 2024a). These measurements facilitate precise studies of the pressure profiles of galaxy clusters, the thermal state of the intracluster medium, and even the temperature of filaments connecting galaxy clusters within the cosmic web. Looking ahead, future CMB surveys such as CMB-S4 promise to significantly expand our understanding of galaxy clusters. With its wide survey covering  $f_{\text{sky}} = 50\%$ , CMB-S4 is expected to detect approximately 75,000 clusters, while its deep survey covering  $f_{\text{sky}} = 3\%$  will detect around 14,000 clusters. Remarkably, about 1,350 of these clusters will be at  $z \geq 2$ , enabling unprecedented studies of cluster evolution at high redshifts (Raghunathan et al., 2022).

### Relativistic tSZ

The relativistic tSZ effect is a generalization of the standard tSZ effect, incorporating corrections that arise due to the high thermal velocities of electrons in galaxy clusters. In the standard tSZ framework, the interaction between the CMB photons and the hot, ionized gas (intra-cluster medium) is treated under the assumption of a non-relativistic electron distribution, where the thermal electron velocities are much smaller than the speed of light. However, in massive clusters ( $M \gtrsim 4 \times 10^{14} M_\odot$ ) with very high temperatures—such as those exceeding 10 keV—this approximation begins to break down, as the electrons exhibit relativistic velocities, i.e.  $v_e = \sqrt{2k_B T_e/m_e} \gtrsim 0.1c$ . These relativistic corrections modify both the amplitude and the frequency dependence of the tSZ spectral distortion (e.g. Wright, 1979; Rephaeli, 1995; Itoh et al., 1998). The relativistic corrections are significant because they affect the spectral shape of the tSZ effect, altering the location and amplitude of the crossover frequency (where the tSZ effect transitions from a decrement to an increment relative to the CMB intensity).

More specifically, Eq. 17 modifies to

$$f(x) = \left( x \frac{e^x + 1}{e^x - 1} - 4 \right) (1 + \delta_{\text{rel}}(x, T_e)), \quad (20)$$

where  $\delta_{\text{rel}}(x, T_e)$  is the relativistic correction to the frequency dependence of tSZ. These corrections are described by higher-order terms in the electron temperature  $k_B T_e / m_e c^2$ .

The relativistic tSZ effect is computed using a more precise treatment of the photon-electron Compton scattering process, accounting for the full relativistic kinematics. This results in a spectral distortion given by a series expansion or more exact numerical integration. The primary impact of these corrections is at higher frequencies ( $\nu > 200$  GHz), where they become essential for accurately modeling the tSZ signal in hot clusters.

Studying the relativistic tSZ effect provides valuable insights into the thermodynamic state of galaxy clusters. Since the magnitude and spectral features of the relativistic corrections depend on the cluster's electron temperature, precise measurements of the tSZ effect across a wide frequency range allow us to probe the temperature distribution of the intracluster medium (e.g., Hurier, 2016; Erler et al., 2018; Coulton et al., 2024a; Remazeilles and Chluba, 2024). This is especially useful for distinguishing between thermal and non-thermal components, as well as for testing cosmological models through the relationship between the cluster gas and total mass.

### 3.1.2 Kinematic SZ

The kSZ effect is caused by the Doppler shift of CMB photons as they scatter off free electrons in the intracluster medium (ICM) of galaxy clusters. Unlike tSZ effect, which arises from the thermal motion of electrons, the kSZ effect results from the bulk peculiar velocity of the cluster relative to the CMB rest frame. This effect introduces a shift in the observed CMB temperature without altering its spectral shape.

The kSZ effect produces a temperature fluctuation  $\Delta T_{\text{kSZ}}$  in the CMB, which is given by:

$$\frac{\Delta T_{\text{kSZ}}}{T_{\text{CMB}}} = - \int n_e e^{-\tau_e} \sigma_T \frac{\mathbf{v} \cdot \hat{\mathbf{n}}}{c} dl, \quad (21)$$

where  $\mathbf{v}$  is the peculiar velocity of the cluster and  $\hat{\mathbf{n}}$  is the unit vector pointing along the line-of-sight. The term  $\mathbf{v} \cdot \hat{\mathbf{n}}$  represents the component of the cluster's peculiar velocity along the observer's line-of-sight ( $v_r$ , or the radial velocity).  $\tau_e$  is the optical depth to Thomson scattering, and the integral accounts for the electron density  $n_e$  along the line-of-sight, weighted by the velocity.

The optical depth,  $\tau_e$ , of a cluster is given by:

$$\tau_e = \int n_e \sigma_T dl, \quad (22)$$

and the kSZ temperature fluctuation simplifies to:

$$\frac{\Delta T_{\text{kSZ}}}{T_{\text{CMB}}} = -\tau_e \frac{v_r}{c}. \quad (23)$$

Unlike the tSZ effect, the kSZ effect preserves the blackbody shape of the CMB spectrum. This means it results in a uniform shift in intensity at all frequencies proportional to the peculiar velocity of the cluster (see Fig. 6). The kSZ signal is challenging to detect because it lacks the distinct spectral signature of the tSZ effect and is typically smaller in magnitude.

The kSZ effect provides unique insights into the large-scale velocity field of the universe (e.g., Deutsch et al., 2018; Smith et al., 2018). By measuring the kSZ signal, we can estimate the peculiar velocities of galaxy clusters, revealing information about the distribution of matter and the LSS dynamics. This is particularly useful for testing cosmological models, including the influence of dark energy and modified gravity on the growth of structure (e.g. DeDeo et al., 2005; Bhattacharya and Kosowsky, 2008; Mueller et al., 2015; Ma and Zhao, 2014; Alonso et al., 2016; Bianchini and Silvestri, 2016), as well as primordial non-Gaussianities (Münchmeyer et al., 2019). Furthermore, kSZ measurements can constrain the baryon content of the universe, as the signal depends on the electron density along the line-of-sight. Combined with weak gravitational lensing and tSZ measurements, the kSZ effect allows for a detailed study of the connection between baryonic and dark matter in galaxy clusters (e.g., Battaglia et al., 2017; Schaan et al., 2021; Amodeo et al., 2021).

Detecting the kSZ effect is challenging due to its small amplitude, contamination from primary CMB anisotropies, and other astrophysical foregrounds. As a result, individual clusters' velocities are currently measured from mm-wave observations for only a small number of objects (e.g., Sayers et al., 2013; Adam et al., 2017). Since the kSZ effect preserves the blackbody spectrum of the primary CMB, it cannot be isolated using standard component separation techniques alone. Instead, the signal is detected by combining CMB data with LSS observations through statistical methods or estimators. Early detections of the kSZ effect were achieved by applying the pairwise momentum method to ACT data combined with BOSS spectroscopic galaxies in 2012 (Hand et al., 2012), followed by additional detections using *Planck*, SPT, and ACT data in conjunction with spectroscopic and photometric LSS samples (Bernardis et al., 2017; Soergel et al., 2016; Calafut et al., 2021; Schiappucci et al., 2023). Velocity-weighted stacking techniques have been employed to constrain baryon density profiles, as demonstrated with ACT data and BOSS galaxies (Schaan et al., 2016; Schaan et al., 2021; Amodeo et al., 2021), and more recently with DESI photometric LRGs (Hadzhiyska et al., 2024). The first detection using velocity reconstruction was recently achieved with ACT data and DESI LRGs (McCarthy et al., 2024). Other classes of estimators that are sensitive to the  $\langle TTg \rangle$  bispectrum (where 'g' represents the galaxy over-density field), also known as projected-fields estimators, involve filtering and squaring CMB maps before cross-correlating with LSS, represent distinct approaches to extracting kSZ signals (e.g., Hill et al., 2016; Kusiak et al., 2021).

Another significant contribution to the kSZ signal originates from the epoch of reionization, where local variations in the ionized fraction

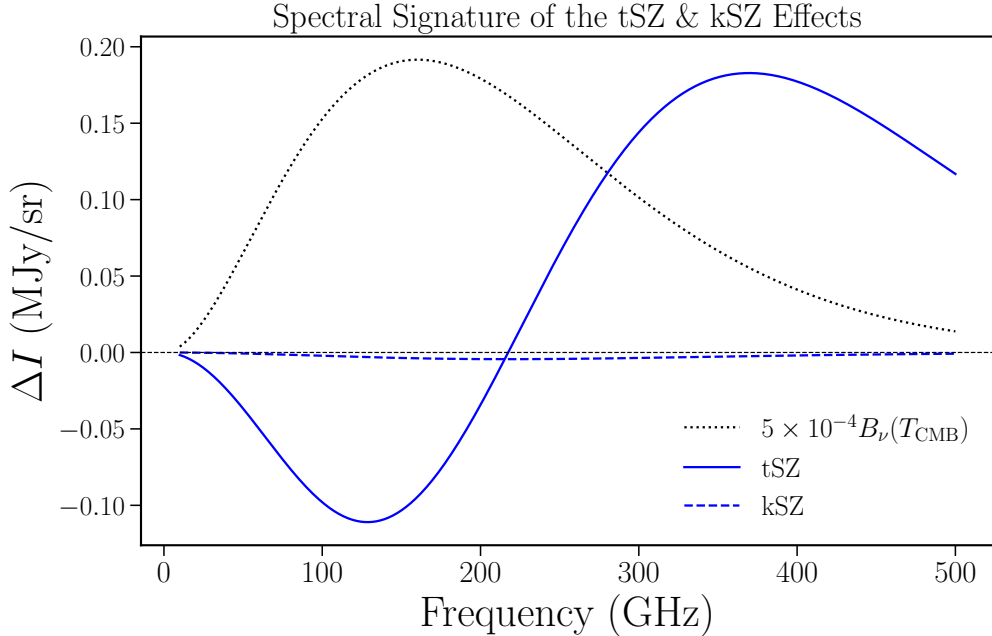


Fig. 6: Frequency-dependent changes in CMB intensity caused by the tSZ (solid blue) and kSZ (dashed blue) effects. The dotted curve represents the thermal CMB spectrum at a temperature of 2.7 K, scaled by a factor of  $5 \times 10^{-4}$ . The kSZ effect preserves the blackbody nature of the CMB spectrum, while the tSZ effect introduces a spectral distortion with a null point around 217 GHz. These curves were generated using a Compton parameter  $y = 10^{-4}$ , a cluster peculiar velocity of 1000 km/s, and an optical depth  $\tau_e = 10^{-3}$ .

and free electron density create arcminute-scale temperature anisotropies in the CMB. This effect is commonly referred to as the “patchy” kSZ effect (e.g., McQuinn et al., 2005; Shaw et al., 2012; Battaglia et al., 2013; Park et al., 2013). Distinguishing the patchy kSZ signal from the low-redshift kSZ contribution is challenging. Smith and Ferraro (2017) proposed using the kSZ trispectrum as a method to isolate the reionization-era contribution. However, recent analyses applying this approach to SPT/Herschel and ACT data have so far only yielded upper limits on the kSZ trispectrum. These studies found that foreground contamination poses a significant obstacle, with foreground signals dominating over the expected kSZ signal (Raghunathan et al., 2024; MacCrann et al., 2024).

#### Rotational kSZ

The rotational kSZ effect is a variant of the kSZ effect that arises from the rotational motion of galaxy clusters. Unlike the standard kSZ effect, which is caused by the bulk peculiar motion of the cluster along the line-of-sight, the rotational kSZ effect originates from the coherent tangential motion of intracluster gas around the center of mass of the cluster. This rotational motion creates a dipole-like pattern in the CMB temperature fluctuations across the cluster, with opposite sides of the cluster showing slightly redshifted and blueshifted signals, respectively, due to the Doppler effect. The amplitude of the rotational kSZ effect is proportional to the rotational velocity of the gas and the optical depth ( $\tau_e$ ). Observing this effect provides a unique way to measure angular momentum in galaxy clusters and to study the dynamics of gas in cluster halos, offering insights into the processes driving the assembly and evolution of large-scale structure. Detecting the rotational kSZ effect, however, is observationally challenging due to its weak signal and the need to separate it from other kSZ contributions and astrophysical foregrounds. For example, Baxter et al. (2019) analyzed *Planck* data using 13 galaxy clusters from SDSS-DR10, reporting approximately  $2\sigma$  evidence of a rotational kSZ signal with an amplitude and morphology consistent with theoretical expectations.

### 3.2 Polarized SZ

While SZ effects predominantly influence the intensity of the CMB, polarization can also occur under specific circumstances. The main sources of SZ polarization are quadrupole anisotropies in the incoming CMB radiation (Sazonov and Sunyaev, 1999) and the peculiar motion of galaxy clusters (Sunyaev and Zeldovich, 1980; Sazonov and Sunyaev, 1999). Quadrupole-induced polarization occurs because the Thomson scattering process imprints the anisotropy of the incoming radiation onto the scattered light. This effect depends on the local CMB quadrupole observed at the location of the scattering electrons and is the dominant source of polarization in SZ. It is typically expected to be on the order of micro-Kelvin or smaller. Detection of this effect could allow measurements of the optical depth  $\tau_e$  of the cluster as it is proportional to  $\tau$  times the tSZ effect. In principle, it could thus separate  $T_e$  and  $\tau_e$  by measuring tSZ (Eq. 16 and 22).

In contrast, motion-induced polarization arises from the relative velocity between the cluster and the observer. This effect is proportional to  $(v_t/c)^2 \tau_e$ , where  $v_t$  is transverse velocity of the cluster. Typically this effect is of the order of nano-Kelvin and is sensitive to the transverse

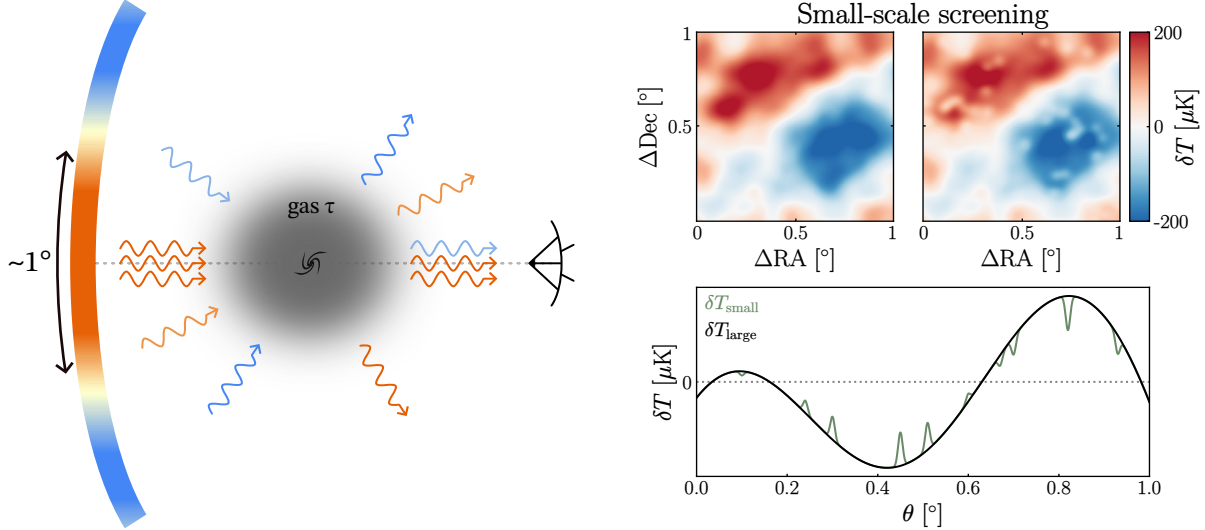


Fig. 7: **Left:** Intuitive understanding of the patchy screening effect. We have photons coming from typical 1 deg CMB fluctuations from left that get Thomson scattered by electrons in gas around a galaxy in the line-of-sight (LOS). As a result, some of these photons are scattered out of the LOS and are replaced by photons from all other directions scattered into our LOS with the temperature averaged across all directions. This has an effect of ‘smoothing’ CMB anisotropies in a given LOS. Credit: Theo Schutt. **Right:** Top- 1 deg<sup>2</sup> simulated map of a CMB realization unscreened (left) and screened by 5° FWHM 2D Gaussian  $\tau$  profiles placed at a fixed realization of galaxy positions in the foreground (right). The  $\tau$  amplitude is greatly exaggerated for visual effect. Bottom- A 1D schematic illustrating the small angular scale temperature deviations  $\delta T_{\text{small}}$  induced by the patchy screening effect (green). Unlike any other foreground, these deviations are (anti-)correlated with the large-scale primary CMB anisotropies  $\delta T_{\text{large}}$  (black). This effectively ‘smooths’ CMB anisotropies bringing the small-scale anisotropies close to the mean of the map as can be seen by comparing the unscreened and screened simulated maps. Plot taken from Schutt et al. (2024).

velocity component of the cluster with respect to our line-of-sight, which is difficult to measure otherwise. The resulting polarization vector is perpendicular to the plane formed by the line-of-sight and the velocity vector.

Two other sources of polarization in SZ are double scattering-induced polarization, and Faraday rotation-induced polarization due to presence of magnetic fields in clusters (e.g. Aghanim et al., 2008). These effects are expected to be smaller than the dominant quadrupole-induced polarization.

Polarization of the SZ effect is typically much weaker than the intensity signals but carries unique information. By detecting and analyzing the polarized SZ signals, cosmologists can probe the dynamics of galaxy clusters, map large-scale velocity fields, and potentially constrain the evolution of the CMB quadrupole, offering insights into early universe physics and large-scale structure evolution.

### 3.3 Patchy screening

Apart from the inverse Compton scattering which gives rise to the SZ effects, CMB photons also undergo Thomson scattering by electrons in gas around galaxies and in clusters. This scattering damps the primary CMB anisotropies and has two components. The isotropic component of this scattering scales with the optical depth to reionization which is one of the six standard parameters of the  $\Lambda$ CDM cosmology (Planck Collaboration et al., 2020b). This relationship connects the observed CMB anisotropies to the intrinsic ones through:

$$\Delta T(\hat{\mathbf{n}}) = \Delta T^0(\hat{\mathbf{n}}) e^{-\tau(\hat{\mathbf{n}})}, \quad (24)$$

where  $\Delta T(\hat{\mathbf{n}})$  and  $\Delta T^0(\hat{\mathbf{n}})$  are the observed and intrinsic CMB temperature anisotropy in a given direction  $\hat{\mathbf{n}}$  respectively, and  $\tau(\hat{\mathbf{n}})$  is the optical depth to Thomson scattering in that patch of the sky. However, the distribution of electrons responsible for this scattering is anisotropic, meaning that some lines of sight contain more electrons than others. This leads to anisotropic damping, which spatially modulates the underlying CMB anisotropies and introduces a new source of small-scale  $\leq 1^\circ$  anisotropies in the CMB maps. This phenomenon is known as “patchy screening” of the CMB photons.

Patchy screening arises from two distinct phases: (1) during the epoch of reionization, when large spatial fluctuations in the ionization fraction were present, and (2) in the late-time Universe ( $z < 5$ ) when gravitationally collapsed objects have large electron overdensities. Consequently, patchy screening traces anisotropies in the optical depth to Thomson scattering, as ionized or collapsed regions are unevenly distributed across the sky. This can be expressed as:  $\tau(\hat{\mathbf{n}}) = \bar{\tau} + \delta\tau(\hat{\mathbf{n}})$ ; where  $\bar{\tau}$  and  $\delta\tau(\hat{\mathbf{n}})$  are the mean and fluctuations in  $\tau$  respectively. Using this in Eq. 24 with  $\delta\tau(\hat{\mathbf{n}}) \ll 1$ , and absorbing  $\bar{\tau}$  in the intrinsic CMB anisotropies gives

$$\Delta T(\hat{\mathbf{n}}) = -\delta\tau(\hat{\mathbf{n}}) \Delta T^0(\hat{\mathbf{n}}). \quad (25)$$

This expression is analogous to Eq. 7 for weak lensing of the CMB. In the Fourier domain, patchy screening, like CMB lensing, couples different modes of the CMB. These mode couplings form the basis for constructing quadratic estimators of the screening field (Dvorkin and Smith, 2009). While Eqs. 24 and 25 are written for CMB temperature maps, they also apply to the  $Q$  and  $U$  polarization maps. Similar to CMB lensing, patchy screening generates a  $B$ -mode polarization signal.

A clear separation of scales emerges in Eq. 25, when considering the effect of screening on small scales. Denoting small and large scales with subscripts S and L respectively, Eq. 25 becomes

$$\Delta T_S(\hat{\mathbf{n}}) = -\delta\tau_S(\hat{\mathbf{n}}) \Delta T_L^0(\hat{\mathbf{n}}), \quad (26)$$

indicating that the screening effect on small scales is almost exclusively sourced by configurations where small-scale variations in the optical depth modulate the large-scale CMB anisotropies. As a result of this separation of scales, Schutt et al. (2024) were able to show that both the screened and unscreened temperature fluctuations can be measured from the same map, and that can give an estimate of patchy screening on small scales. This effect is illustrated in the bottom-right panel of Fig. 7, which shows how small-scale CMB anisotropies due to screening arise from the modulation of large-scale CMB anisotropies by small-scale screening. Additionally, as seen from Eqs. 25 and 26, the sign of the screening anisotropy is always opposite to the sign of the corresponding large-scale CMB anisotropy in the same patch of sky. This implies that screening effectively “smooths” the CMB anisotropies in a given region, bringing them closer to the mean. This smoothing effect can be observed in the top-right panel of Fig. 7, where the left and right simulated maps illustrate the unscreened and screened CMB anisotropies, respectively.

Finally, since patchy screening receives contributions from the epoch of reionization, it provides a valuable tool for studying the mechanisms of reionization. The patchy screening signal is sensitive to the morphology and timing of reionization, including the size and distribution of ionized bubbles, the nature of ionizing sources, and the properties of the surrounding IGM. By analyzing this effect, we can infer key aspects of the history of reionization, such as its onset and the timescale over which it progressed (e.g., Roy et al., 2018; Namikawa et al., 2021; Ade et al., 2023; Bianchini and Millea, 2023). In addition, since the damping caused by screening is proportional to the free electrons overdensity, the low redshift contribution to screening is an excellent probe of the gas in the circumgalactic medium (e.g. Roy et al., 2023; Schutt et al., 2024; Coulton et al., 2024b). The amplitude and angular scale of the patchy screening signal directly trace the projected gas profile, making screening a complementary probe to the kSZ effect, which also studies gas around galaxies. Similar to the tSZ effect, patchy screening is independent of redshift, making it a powerful tool for probing gas properties across a wide range of cosmic epochs, from low to high redshifts.

## 4 Concluding Remarks

In this chapter, we have explored the physical mechanisms behind secondary anisotropies in the CMB and reviewed their current observational status and future prospects. Secondary anisotropies arise from two broad classes of effects, categorized by their underlying sourcing mechanisms: gravitational and scattering. As CMB photons journey from the surface of last scattering to us, they interact with the LSS of the universe, providing a unique backlight that enables the imaging of both gravitational potentials and the gas distribution in the universe. Gravitational effects such as weak gravitational lensing, the ISW effect, and the RS and ML effects allow us to probe the distribution and evolution of matter and gravitational potentials. Scattering effects, such as those caused by Thomson and inverse Compton scattering, include the tSZ and kSZ effects, as well as patchy screening, which provide valuable insights into the distribution, temperature, and motion of ionized gas in the universe.

This is an exciting time for CMB research, as the current generation of surveys—including *Planck* (Planck Collaboration et al., 2020a), SPT (Reichardt et al., 2020), and ACT (Aiola et al., 2020)—have begun to unlock the vast potential of secondary CMB anisotropies. These experiments have demonstrated the power of CMB maps to shed light on both cosmological and astrophysical phenomena, laying the foundation for the next generation of surveys. Upcoming experiments such as the Simons Observatory (Ade et al., 2019), FYST/CCAT-prime (Aravena et al., 2019), and CMB-S4 (Abazajian et al., 2022) promise to deliver transformative advancements. With their higher sensitivity, improved resolution, and broader frequency coverage, these surveys will provide a high-fidelity view of secondary anisotropies in both intensity and polarization. This unprecedented precision will enable us to probe fundamental physics and astrophysics in ways previously unattainable.

One particularly exciting frontier is the synergy between CMB and LSS surveys (Baxter et al., 2022). The combination of these complementary probes will enable robust cross-correlation analyses, yielding tighter and more robust constraints on key questions in both cosmology and astrophysics. For example, these analyses will improve our understanding of the equation of state of dark energy, primordial non-Gaussianity, and the physics of galaxy biasing, intrinsic alignments, and baryonic feedback processes. The expected science return from these cross-correlation studies is multi-faceted, offering insights into both fundamental physics and the interplay of matter and radiation in the universe. To fully capitalize on these opportunities, significant efforts are required to develop improved theoretical models and correlated simulations that can match the precision of these upcoming datasets. Work in this direction has already begun (e.g., Stein et al., 2020; Han et al., 2021; Omori, 2024; Bayer et al., 2024), but continued advancements will be essential for ensuring robust and unbiased analyses.

In summary, the study of secondary CMB anisotropies represents a rapidly evolving field that bridges cosmology and astrophysics. Current and next-generation experiments, along with advances in theory and simulations, will further solidify the role of CMB secondary anisotropies as a cornerstone of precision cosmology and a window into the underlying structure and dynamics of the universe.

## Acknowledgments

We dedicate this chapter to the memory of Eric Baxter, whose contributions to this field and to the study of secondary anisotropies were both profound and inspiring. Eric was a brilliant researcher and a wonderful colleague, and his presence in our community is deeply missed. We also thank Yuuki Omori, Emmanuel Schaan, Theo Schutt, and Zuoqi Zhang for their valuable feedback and for providing material that greatly enhanced this work. FB acknowledges support by the Department of Energy, Contract DE-AC02-76SF00515.

## References

- Abazajian K and et al. (CMB-S4) (2022), 3. Snowmass 2021 CMB-S4 White Paper 2203.08024.
- Abbott TMC, Abdalla FB, Alarcon A, Allam S, Annis J, Avila S, Aylor K, Banerji M, Banik N, Baxter EJ, Bechtol K, Becker MR, Benson BA, Bernstein GM, Bertin E, Bianchini F, Blazek J, Bleem LE, Bridle SL, Brooks D, Buckley-Geer E, Burke DL, Carlstrom JE, Carnero Rosell A, Carrasco Kind M, Carretero J, Castander FJ, Cawthon R, Chang C, Chang CL, Cho HM, Choi A, Chown R, Crawford TM, Crites AT, Crocce M, Cunha CE, D'Andrea CB, da Costa LN, Davis C, de Haan T, DeRose J, Desai S, De Vicente J, Diehl HT, Dietrich JP, Dobbs MA, Dodelson S, Doel P, Drlica-Wagner A, Eifler TF, Elvin-Poole J, Everett WB, Flaugher B, Fosalba P, Friedrich O, Frieman J, García-Bellido J, Gatti M, Gaztanaga E, George EM, Gerdes DW, Giannantonio T, Gruen D, Gruendl RA, Gschwend J, Gutierrez G, Halverson NW, Harrington NL, Hartley WG, Holder GP, Hollowood DL, Holzapfel WL, Honscheid K, Hou Z, Hoyle B, Hrubes JD, Huterer D, Jain B, James DJ, Jarvis M, Jeltema T, Johnson MWG, Johnson MD, Kent S, Kirk D, Knox L, Kokron N, Krause E, Kuehn K, Lahav O, Lee AT, Leitch EM, Li TS, Lima M, Lin H, Luong-Van D, MacCrann N, Maia MAG, Manzotti A, Marrone DP, Marshall JL, Martini P, McMahon JJ, Menanteau F, Meyer SS, Miquel R, Mocanu LM, Mohr JJ, Muir J, Natoli T, Nicola A, Nord B, Omori Y, Padin S, Pandey S, Plazas AA, Porredon A, Prat J, Pryke C, Rau MM, Reichardt CL, Rollins RP, Romer AK, Roodman A, Ross AJ, Rozo E, Ruhl JE, Rykoff ES, Samuroff S, Sánchez C, Sanchez E, Sayre JT, Scarpine V, Schaffer KK, Secco LF, Serrano S, Sevilla-Noarbe I, Sheldon E, Shirokoff E, Simard G, Smith M, Soares-Santos M, Sobreira F, Staniszewski Z, Stark AA, Story KT, Suchtya E, Swanson MEC, Tarle G, Thomas D, Troxel MA, Tucker DL, Vanderlinde K, Vieira JD, Vielzeuf P, Vikram V, Walker AR, Wechsler RH, Weller J, Williamson R, Wu WLK, Yanny B, Zahn O, Zhang Y, Zuntz J, DES and SPT Collaborations (2019), Jul. Dark Energy Survey year 1 results: Joint analysis of galaxy clustering, galaxy lensing, and CMB lensing two-point functions. *Phys. Rev. D* 100 (2), 023541. doi:10.1103/PhysRevD.100.023541. 1810.02322.
- Acquaviva V and Baccigalupi C (2006), nov. Dark energy records in lensed cosmic microwave background. *Physical Review D* 74 (10): 103510. ISSN 1550-7998. doi:10.1103/PhysRevD.74.103510. 0507644v2, <http://link.aps.org/doi/10.1103/PhysRevD.74.103510>.
- Adam R, Bartalucci I, Pratt GW, Ade P, André P, Arnaud M, Beelen A, Benoît A, Bideaud A, Billot N and et al. (2017), Feb. Mapping the kinetic sunyaev-zel'dovich effect toward macs j0717.5+3745 with nika. *Astronomy & Astrophysics* 598: A115. ISSN 1432-0746. doi:10.1051/0004-6361/201629182. <http://dx.doi.org/10.1051/0004-6361/201629182>.
- Ade PAR, Aghanim N, Arnaud M, Ashdown M, Aumont J, Baccigalupi C, Banday AJ, Barreiro RB, Bartolo N, Basak S, Battaner E, Benabed K, Benoit A, Benoit-Lévy A, Bernard JP, Bersanelli M, Bielewicz P, Bock JJ, Bonaldi A, Bonavera L, Bond JR, Borrill J, Bouchet FR, Bucher M, Burigana C, Butler RC, Calabrese E, Cardoso JF, Casaponsa B, Catalano A, Challinor A, Chamballu A, Chiang HC, Christensen PR, Church S, Clements DL, Colombi S, Colombo LPL, Combet C, Couchot F, Coulais A, Crill BP, Curto A, Cuttaia F, Danese L, Davies RD, Davis RJ, de Bernardis P, de Rosa A, de Zotti G, Delabrouille J, Désert FX, Diego JM, Dole H, Donzelli S, Doré O, Doussis M, Ducout A, Dupac X, Efstathiou G, Elsner F, Enßlin TA, Eriksen HK, Ferguson J, Fernandez-Cobos R, Finelli F, Forni O, Frailis M, Fraisse AA, Franceschi E, Frejsel A, Galeotta S, Galli S, Ganga K, Génova-Santos RT, Giard M, Giraud-Héraud Y, Gjerløw E, González-Nuevo J, Górski KM, Gratton S, Gregorio A, Gruppuso A, Gudmundsson JE, Hansen FK, Hanson D, Harrison DL, Henrot-Versillé S, Hernández-Monteagudo C, Herranz D, Hildebrandt SR, Hivon E, Hobson M, Holmes WA, Hornstrup A, Hovest W, Huffenberger KM, Hurier G, Ilić S, Jaffe AH, Jaffe TR, Jones WC, Juvela M, Keihänen E, Keskitalo R, Kisner TS, Kneissl R, Knoche J, Kunz M, Kurki-Suonio H, Lagache G, Lähteenmäki A, Lamarre JM, Langer M, Lasenby A, Lattanzi M, Lawrence CR, Leonardi R, Lesgourgues J, Levrier F, Liguori M, Lilje PB, Linden-Vørnle M, López-Caniego M, Lubin PM, Ma YZ, Macías-Pérez JF, Maggio G, Maino D, Mandolesi N, Mangilli A, Marcos-Caballero A, Maris M, Martin PG, Martínez-González E, Masi S, Matarrese S, McGeehee P, Meinhold PR, Melchiorri A, Mendes L, Mennella A, Migliaccio M, Mitra S, Miville-Deschénes MA, Moneti A, Montier L, Morgante G, Mortlock D, Moss A, Munshi D, Murphy JA, Naselsky P, Natli F, Natoli P, Netterfield CB, Nørgaard-Nielsen HU, Noviello F, Novikov D, Novikov I, Oxburrow CA, Paci F, Pagano L, Pajot F, Paoletti D, Pasian F, Patanchon G, Perdereau O, Perotto L, Perrotta F, Pettorino V, Piacentini F, Piat M, Pierpaoli E, Pietrobon D, Plaszczynski S, Pointecouteau E, Polenta G, Popa L, Pratt GW, Prézeau G, Prunet S, Puget JL, Rachen JP, Reach WT, Rebolo R, Reinecke M, Remazeilles M, Renault C, Renzi A, Ristorcelli I, Rocha G, Rosset C, Rossetti M, Roudier G, Rubiño-Martín JA, Rusholme B, Sandri M, Santos D, Savelainen M, Savini G, Schaefer BM, Scott D, Seiffert MD, Shellard EPS, Spencer LD, Stolyarov V, Stompor R, Sudíwala R, Sunyaev R, Sutton D, Suur-Uiski AS, Sygnet JF, Tauber JA, Terenzi L, Toffolatti L, Tomasi M, Tristram M, Tucci M, Tuovinen J, Valenziano L, Valiviita J, Van Tent F, Vielva P, Villa F, Wade LA, Wandelt BD, Wehus IK, Yvon D, Zacchei A and Zonca A (2016), Sep. Planck2015 results: Xxi. the integrated sachs-wolfe effect. *Astronomy& Astrophysics* 594: A21. ISSN 1432-0746. doi:10.1051/0004-6361/201525831. <http://dx.doi.org/10.1051/0004-6361/201525831>.
- Ade P, Aguirre J, Ahmed Z, Aiola S, Ali A, Alonso D, Alvarez MA, Arnold K, Ashton P, Austermann J, Awan H, Baccigalupi C, Baillod T, Barron D, Battaglia N, Battye R, Baxter E, Bazarko A, Beall JA, Bean R, Beck D, Beckman S, Beringue B, Bianchini F, Boada S, Boettger D, Bond JR, Borrill J, Brown ML, Bruno SM, Bryan S, Calabrese E, Calafut V, Calisse P, Carron J, Challinor A, Chesmore G, Chinone Y, Chluba J, Cho HMS, Choi S, Coppi G, Cothard NF, Coughlin K, Crichton D, Crowley KD, Crowley KT, Cukierman A, D'Ewart JM, Dünner R, de Haan T, Devlin M, Dicker S, Didier J, Dobbs M, Dober B, Duell CJ, Duff S, Duivenvoorden A, Dunkley J, Dusatko J, Errard J, Fabbian G, Feeney S, Ferraro S, Fluxà P, Freese K, Frisch JC, Frolov A, Fuller G, Fuzia B, Galitzki N, Gallardo PA, Tomas Galvez Gherisi J, Gao J, Gawiser E, Gerbino M, Gluscevic V, Goeckner-Wald N, Golec J, Gordon S, Gralla M, Green D, Grigorian A, Groh J, Groppi C, Guan Y, Gudmundsson JE, Han D, Hargrave P, Hasegawa M, Hasselfield M, Hattori M, Haynes V, Hazumi M, He Y, Healy E, Henderson SW, Hervias-Caimapo C, Hill CA, Hill JC, Hilton G, Hilton M, Hincks AD, Hinshaw G, Hložek R, Ho S, Ho SPP, Howe L, Huang Z, Hubmayr J, Huffenberger K, Hughes JP, Iijas A, Ikape M, Irwin K, Jaffe AH, Jain B, Jeong O, Kaneko D, Karpel ED, Katayama N, Keating B, Kernasovskiy SS, Keskitalo R, Kisner T, Kiuchi K, Klein J, Knowles K, Koopman B, Kosowsky A, Krachmalnicoff N, Kuenster SE, Kuo CL, Kusaka A, Lashner J, Lee A, Lee E, Leon D, Leung JSY, Lewis A, Li Y, Li Z, Limon M, Linder E, Lopez-Caraballo C, Louis T, Lowry L, Lungu M, Madhavacheril M, Mak D, Maldonado F, Mani H, Mates B, Matsuda F, Maurin L, Mauskopf P, May A, McCallum N, McKenney C, McMahon J, Meerburg PD, Meyers J, Miller A, Mirmelstein M, Moodley K, Munchmeyer M, Munson C, Naess S, Natli F, Navaroli M, Newburgh L, Nguyen HN, Niemack M, Nishino H, Orlowski-Scherer J, Page L, Partridge B, Peloton J, Perrotta F, Piccirillo L, Pisano G, Poletti D, Puddu R, Puglisi G, Raum C, Reichardt CL, Remazeilles M,

- Rephaeli Y, Riechers D, Rojas F, Roy A, Sadeh S, Sakurai Y, Salatino M, Sathyarayana Rao M, Schaan E, Schmittfull M, Sehgal N, Seibert J, Seljak U, Sherwin B, Shimon M, Sierra C, Sievers J, Sikhsana P, Silva-Feaver M, Simon SM, Sinclair A, Siritanasak P, Smith K, Smith SR, Spergel D, Staggs ST, Stein G, Stevens JR, Stompor R, Suzuki A, Tajima O, Takakura S, Teply G, Thomas DB, Thorne B, Thornton R, Trac H, Tsai C, Tucker C, Ullom J, Vagnozzi S, van Engelen A, Van Lanen J, Van Winkle DD, Vavagiakis EM, Vergès C, Vissers M, Wagoner K, Walker S, Ward J, Westbrook B, Whitehorn N, Williams J, Williams J, Wollack EJ, Xu Z, Yu B, Yu C, Zago F, Zhang H, Zhu N and Simons Observatory Collaboration (2019), Feb. The Simons Observatory: science goals and forecasts. *J. Cosmol. Astropart. Phys.* 2019 (2), 056. doi:10.1088/1475-7516/2019/02/056. 1808.07445.
- Ade PAR and et al. (BICEP/Keck) (2023). BICEP/Keck. XVII. Line-of-sight Distortion Analysis: Estimates of Gravitational Lensing, Anisotropic Cosmic Birefringence, Patchy Reionization, and Systematic Errors. *Astrophys. J.* 949 (2): 43. doi:10.3847/1538-4357/accc85c. 2210.08038.
- Aghanim N, Majumdar S and Silk J (2008), May. Secondary anisotropies of the cmb. *Reports on Progress in Physics* 71 (6): 066902. ISSN 1361-6633. doi:10.1088/0034-4885/71/6/066902. <http://dx.doi.org/10.1088/0034-4885/71/6/066902>.
- Aiola S, Calabrese E, Maurin L, Naess S, Schmitt BL, Abitbol MH, Addison GE, Ade PAR, Alonso D, Amiri M, Amodeo S, Angile E, Austermann JE, Baillod T, Battaglia N, Beall JA, Bean R, Becker DT, Bond JR, Bruno SM, Calafut V, Campusano LE, Carrero F, Chesmore GE, Cho Hm, Choi SK, Clark SE, Cothard NF, Crichton D, Crowley KT, Darwish O, Datta R, Denison EV, Devlin MJ, Duell CJ, Duff SM, Duivenvoorden AJ, Dunkley J, Dünner R, Essinger-Hileman T, Fankhanel M, Ferraro S, Fox AE, Fuzia B, Gallardo PA, Gluscevic V, Golec JE, Grace E, Gralla M, Guan Y, Hall K, Halpern M, Han D, Hargrave P, Hasselfield M, Helton JM, Henderson S, Hensley B, Hill JC, Hilton GC, Hilton M, Hincks AD, Hložek R, Ho SPP, Hubmayr J, Huffenberger KM, Hughes JP, Infante L, Irwin K, Jackson R, Klein J, Knowles K, Koopman B, Kosowsky A, Lakey V, Li D, Li Y, Li Z, Lokken M, Louis T, Lungu M, Maclnnis A, Madhavacheril M, Maldonado F, Mallaby-Kay M, Marsden D, McMahon J, Menanteau F, Moodley K, Morton T, Namikawa T, Nati F, Newburgh L, Nibarger JP, Nicola A, Niemack MD, Nolta MR, Orlowski-Sherer J, Page LA, Pappas CG, Partridge B, Phakathi P, Prince H, Puddu R, Qu FJ, Rivera J, Robertson N, Rojas F, Salatino M, Schaan E, Schillaci A, Sehgal N, Sherwin BD, Sierra C, Sievers J, Sifon C, Sikhsana P, Simon S, Spergel DN, Staggs ST, Stevens J, Storer E, Sunder DD, Switzer ER, Thorne B, Thornton R, Trac H, Treu J, Tucker C, Vale LR, Van Engelen A, Van Lanen J, Vavagiakis EM, Wagoner K, Wang Y, Ward JT, Wollack EJ, Xu Z, Zago F and Zhu N (2020), Jul. The Atacama Cosmology Telescope: DR4 Maps and Cosmological Parameters. *arXiv e-prints*, arXiv:2007.07288v007.07288.
- Alonso D, Louis T, Bull P and Ferreira PG (2016), Aug. Reconstructing cosmic growth with kinetic Sunyaev-Zel'dovich observations in the era of stage IV experiments. *Phys. Rev. D* 94 (4), 043522. doi:10.1103/PhysRevD.94.043522. 1604.01382.
- Alonso D, Fabbian G, Storey-Fisher K, Eilers AC, García-García C, Hogg DW and Rix HW (2023). Constraining cosmology with the Gaia-unWISE Quasar Catalog and CMB lensing: structure growth. *JCAP* 11: 043. doi:10.1088/1475-7516/2023/11/043. 2306.17748.
- Amodeo S, Battaglia N, Schaan E, Ferraro S, Moser E, Aiola S, Austermann JE, Beall JA, Bean R, Becker DT, Bond RJ, Calabrese E, Calafut V, Choi SK, Denison EV, Devlin M, Duff SM, Duivenvoorden AJ, Dunkley J, Dünner R, Gallardo PA, Hall KR, Han D, Hill JC, Hilton GC, Hilton M, Hložek R, Hubmayr J, Huffenberger KM, Hughes JP, Koopman BJ, Maclnnis A, McMahon J, Madhavacheril MS, Moodley K, Mroczkowski T, Naess S, Nati F, Newburgh LB, Niemack MD, Page LA, Partridge B, Schillaci A, Sehgal N, Sifón C, Spergel DN, Staggs S, Storer ER, Ullom JN, Vale LR, van Engelen A, Van Lanen J, Vavagiakis EM, Wollack EJ and Xu Z (2021), Mar. Atacama Cosmology Telescope: Modeling the gas thermodynamics in BOSS CMASS galaxies from kinematic and thermal Sunyaev-Zel'dovich measurements. *Phys. Rev. D* 103 (6), 063514. doi:10.1103/PhysRevD.103.063514. 2009.05558.
- Amon A and Efstathiou G (2022), Sep. A non-linear solution to the s8 tension? *Monthly Notices of the Royal Astronomical Society* 516 (4): 5355–5366. ISSN 1365-2966. doi:10.1093/mnras/stac2429. <http://dx.doi.org/10.1093/mnras/stac2429>.
- Ansarinejad B and et al. (SPT-3G, DES) (2024). Mass calibration of DES Year-3 clusters via SPT-3G CMB cluster lensing. *JCAP* 07: 024. doi:10.1088/1475-7516/2024/07/024. 2404.02153.
- Aravena M, Austermann J, Basu K, Battaglia N, Beringue B, Bertoldi F, Bond JR, Breyses P, Bustos R, Chapman S, Choi S, Chung D, Cothard N, Dober B, Duell C, Duff S, Dunner R, Erler J, Fich M, Fissel L, Foreman S, Gallardo P, Gao J, Giovanelli R, Graf U, Haynes M, Herter T, Hilton G, Hložek R, Hubmayr J, Johnstone D, Keating L, Komatsu E, Magnelli B, Mauskopf P, McMahon J, Meerburg PD, Meyers J, Murray N, Niemack M, Nikola T, Nolta M, Parshley S, Puddu R, Riechers D, Rosolowsky E, Simon S, Stacey G, Stevens J, Stutzki J, Van Engelen A, Vavagiakis E, Viero M, Vissers M, Walker S and Zou B (2019), Sep. The CCAT-Prime Submillimeter Observatory. *arXiv e-prints*, arXiv:1909.02587v1909.02587.
- Bardeen JM (1980). Gauge Invariant Cosmological Perturbations. *Phys. Rev. D* 22: 1882–1905. doi:10.1103/PhysRevD.22.1882.
- Battaglia N, Natarajan A, Trac H, Cen R and Loeb A (2013), Oct. Reionization on Large Scales. III. Predictions for Low-I Cosmic Microwave Background Polarization and High-I Kinetic Sunyaev-Zel'dovich Observables. *Astrophys. J.* 776, 83. doi:10.1088/0004-637X/776/2/83. 1211.2832.
- Battaglia N, Ferraro S, Schaan E and Spergel D (2017). Future constraints on halo thermodynamics from combined Sunyaev-Zel'dovich measurements. *JCAP* 11: 040. doi:10.1088/1475-7516/2017/11/040. 1705.05881.
- Baxter EJ, Keisler R, Dodelson S, Aird KA, Allen SW, Ashby MLN, Bautz M, Bayliss M, Benson BA, Bleem LE, Bocquet S, Brodin M, Carlstrom JE, Chang CL, Chiu I, Cho HM, Clocchiatti A, Crawford TM, Crites AT, Desai S, Dietrich JP, de Haan T, Dobbs MA, Foley RJ, Forman WR, George EM, Gladders MD, Gonzalez AH, Halverson NW, Harrington NL, Hennig C, Hoekstra H, Holder GP, Holzapfel WL, Hou Z, Hrubes JD, Jones C, Knox L, Lee AT, Leitch EM, Liu J, Lueker M, Luong-Van D, Mantz A, Marrone DP, McDonald M, McMahon JJ, Meyer SS, Millea M, Mocanu LM, Murray SS, Padin S, Pryke C, Reichardt CL, Rest A, Ruhl JE, Saliwanchik BR, Saro A, Sayre JT, Schaffer KK, Shirokoff E, Song J, Spieler HG, Stalder B, Stanford SA, Staniszewski Z, Stark AA, Story KT, van Engelen A, Vanderlinde K, Vieira JD, Vikhlinin A, Williamson R, Zahn O and Zenteno A (2015), Jun. A Measurement of Gravitational Lensing of the Cosmic Microwave Background by Galaxy Clusters Using Data from the South Pole Telescope. *Astrophys. J.* 806, 247. doi:10.1088/0004-637X/806/2/247. 1412.7521.
- Baxter EJ, Sherwin BD and Raghunathan S (2019), Jun. Constraining the rotational kinematic sunyaev-zel'dovich effect in massive galaxy clusters. *Journal of Cosmology and Astroparticle Physics* 2019 (06): 001–001. ISSN 1475-7516. doi:10.1088/1475-7516/2019/06/001. <http://dx.doi.org/10.1088/1475-7516/2019/06/001>.
- Baxter EJ, Chang C, Hearin A, Blazek J, Bleem LE, Ferraro S, Ishak M, Karkare KS, Leauthaud A, Liu J, Mandelbaum R, Meyers J, Dizgah AM, Nagai D, Newman JA, Omori Y, Sehgal N, White M, Zuntz J, Alvarez MA, Avestruz C, Bianchini F, Bocquet S, Bolliet B, Carlstrom JE, Doux C, van Engelen A, Goh T, Grandis S, Hill JC, von der Linden A, Maniyar AS, Marques GA, Porredon A, Prat J, Robertson N, Schaan E, Shaikh S, hyeon Shin T and Zhang Y (2022). Snowmass2021: Opportunities from cross-survey analyses of static probes. 2203.06795. <https://arxiv.org/abs/2203.06795>.
- Bayer AE, Zhong Y, Li Z, DeRose J, Feng Y and Liu J (2024). The halfdome multi-survey cosmological simulations: N-body simulations. 2407.17462, <https://arxiv.org/abs/2407.17462>.
- Beck D, Fabbian G and Errard J (2018), Aug. Lensing reconstruction in post-Born cosmic microwave background weak lensing. *Phys. Rev. D* 98, 043512. doi:10.1103/PhysRevD.98.043512. 1806.01216.
- Bernardeau F (1997), Aug. Weak lensing detection in CMB maps. *Astron. Astrophys.* 324: 15–26. arXiv:astro-ph/9611012.
- Bernardis FD, Aiola S, Vavagiakis E, Battaglia N, Niemack M, Beall J, Becker D, Bond J, Calabrese E, Cho H and et al. (2017), Mar. Detection of the pairwise kinematic sunyaev-zel'dovich effect with boss dr11 and the atacama cosmology tele-

- scope. *Journal of Cosmology and Astroparticle Physics* 2017 (03): 008?008. ISSN 1475-7516. doi:10.1088/1475-7516/2017/03/008. <http://dx.doi.org/10.1088/1475-7516/2017/03/008>.
- Bhattacharya S and Kosowsky A (2008). Dark Energy Constraints from Galaxy Cluster Peculiar Velocities. *Phys. Rev. D* 77: 083004. doi: 10.1103/PhysRevD.77.083004. [0712.0034](#).
- Bianchini F and Millea M (2023), Feb. Inference of gravitational lensing and patchy reionization with future cmb data. *Physical Review D* 107 (4). ISSN 2470-0029. doi:10.1103/physrevd.107.043521. <http://dx.doi.org/10.1103/PhysRevD.107.043521>.
- Bianchini F and Reichardt CL (2018), Jul. Constraining gravity at large scales with the 2mass photometric redshift catalog and planck lensing. *The Astrophysical Journal* 862 (1): 81. ISSN 1538-4357. doi:10.3847/1538-4357/aacaf. <http://dx.doi.org/10.3847/1538-4357/aacaf>.
- Bianchini F and Silvestri A (2016), Mar. Kinetic sunyaev-zel'dovich effect in modified gravity. *Physical Review D* 93 (6). ISSN 2470-0029. doi: 10.1103/physrevd.93.064026. <http://dx.doi.org/10.1103/PhysRevD.93.064026>.
- Bianchini F, Bielewicz P, Lapi A, Gonzalez-Nuevo J, Baccigalupi C, de Zotti G, Danese L, Bourne N, Cooray A, Dunne L, Dye S, Eales S, Ivison R, Maddox S, Negrello M, Scott D, Smith MWL and Valiante E (2015), Mar. Cross-correlation between the cmb lensing potential measured by planck and high-zsubmillimeter galaxies detected by the herschel-atlas survey. *The Astrophysical Journal* 802 (1): 64. ISSN 1538-4357. doi:10.1088/0004-637X/802/1/64. <http://dx.doi.org/10.1088/0004-637X/802/1/64>.
- Birkinshaw M (1999). The sunyaev zel'dovich effect. *Physics Reports* 310: 97.
- Birkinshaw M and Gull SF (1983), Mar. A test for transverse motions of clusters of galaxies. *Nature* 302 (5906): 315–317. doi:10.1038/302315a0.
- Blanchard A and Schneider J (1987). Gravitational lensing effect on the fluctuations of the cosmic background radiation. *Astronomy and Astrophysics* 184: 1–6. ISSN 0004-6361.
- Bleem LE, Stalder B, de Haan T, Aird KA, Allen SW, Applegate DE, Ashby MLN, Bautz M, Bayliss M, Benson BA, Bocquet S, Brodin M, Carlstrom JE, Chang CL, Chiu I, Cho HM, Clocchiatti A, Crawford TM, Crites AT, Desai S, Dietrich JP, Dobbs MA, Foley RJ, Forman WR, George EM, Gladders MD, Gonzalez AH, Halverson NW, Hennig C, Hoekstra H, Holder GP, Holzapfel WL, Hrubes JD, Jones C, Keisler R, Knox L, Lee AT, Leitch EM, Liu J, Lueker M, Luong-Van D, Mantz A, Marrone DP, McDonald M, McMahon JJ, Meyer SS, Mocanu L, Mohr JJ, Murray SS, Padin S, Pryke C, Reichardt CL, Rest A, Ruel J, Ruhl JE, Saliwanchik BR, Saro A, Sayre JT, Schaffer KK, Schrabbach T, Shirokoff E, Song J, Spieler HG, Stanford SA, Staniszewski Z, Stark AA, Story KT, Stubbs CW, Vanderlinde K, Vieira JD, Vikhlinin A, Williamson R, Zahn O and Zenteno A (2015), Feb. Galaxy Clusters Discovered via the Sunyaev-Zel'dovich Effect in the 2500-Square-Degree SPT-SZ Survey. *Astrophys. J. Suppl. Ser.* 216, 27. doi:10.1088/0067-0049/216/2/27. [1409.0850](#).
- Bleem LE, Bocquet S, Stalder B, Gladders MD, Ade PAR, Allen SW, Anderson AJ, Annis J, Ashby MLN, Austermann JE, Avila S, Avva JS, Bayliss M, Beall JA, Bechtol K, Bender AN, Benson BA, Bertin E, Bianchini F, Blake C, Brodin M, Brooks D, Buckley-Geer E, Burke DL, Carlstrom JE, Rosell AC, Carrasco Kind M, Carretero J, Chang CL, Chiang HC, Citron R, Moran CC, Costanzi M, Crawford TM, Crites AT, da Costa LN, de Haan T, De Vicente J, Desai S, Diehl HT, Dietrich JP, Dobbs MA, Eifler TF, Everett W, Flaugher B, Floyd B, Frieman J, Gallicchio J, Garcia-Bellido J, George EM, Gerdes DW, Gilbert A, Gruen D, Gruendl RA, Gschwend J, Gupta N, Gutierrez G, Halverson NW, Harrington N, Henning JW, Heymans C, Holder GP, Hollowood DL, Holzapfel WL, Honscheid K, Hrubes JD, Huang N, Hubmayr J, Irwin KD, James DJ, Jeltema T, Joudaki S, Khullar G, Klein M, Knox L, Kuropatkin N, Lee AT, Li D, Lidman C, Lowitz A, MacCrann N, Mahler G, Maia MAG, Marshall JL, McDonald M, McMahon JJ, Melchior P, Menanteau F, Meyer SS, Miquel R, Mocanu LM, Mohr JJ, Montgomery J, Nadolski A, Natoli T, Nibarger JP, Noble G, Novosad V, Padin S, Palmese A, Parkinson D, Patil S, Paz-Chinchón F, Plazas AA, Pryke C, Ramachandra NS, Reichardt CL, Remolina González JD, Romer AK, Roodman A, Ruhl JE, Rykoff ES, Saliwanchik BR, Sanchez E, Saro A, Sayre JT, Schaffer KK, Schrabbach T, Serrano S, Sharon K, Sievers C, Smecher G, Smith M, Soares-Santos M, Stark AA, Story KT, Suchyta E, Tarle G, Tucker C, Vanderlinde K, Veatch T, Vieira JD, Wang G, Weller J, Whitehorn N, Wu WLK, Yefremenko V and Zhang Y (2020), Mar. The SPTpol Extended Cluster Survey. *Astrophys. J. Suppl. Ser.* 247 (1), 25. doi:10.3847/1538-4365/ab6993. [1910.04121](#).
- Bleem LE, Crawford TM, Ansarinejad B, Benson BA, Bocquet S, Carlstrom JE, Chang CL, Chown R, Crites AT, de Haan T, Dobbs MA, Everett WB, George EM, Gualtieri R, Halverson NW, Holder GP, Holzapfel WL, Hrubes JD, Knox L, Lee AT, Luong-Van D, Marrone DP, McMahon JJ, Meyer SS, Millea M, Mocanu LM, Mohr JJ, Natoli T, Omori Y, Padin S, Pryke C, Raghunathan S, Reichardt CL, Ruhl JE, Schaffer KK, Shirokoff E, Staniszewski Z, Stark AA, Vieira JD and Williamson R (2022), Feb. CMB/kSZ and Compton-y Maps from 2500 deg<sup>2</sup> of SPT-SZ and Planck Survey Data. *Astrophys. J. Suppl. Ser.* 258 (2), 36. doi:10.3847/1538-4365/ac35e9. [2102.05033](#).
- Bocquet S, Dietrich JP, Schrabbach T, Bleem LE, Klein M, Allen SW, Applegate DE, Ashby MLN, Bautz M, Bayliss M, Benson BA, Brodin M, Bulbul E, Canning REA, Capasso R, Carlstrom JE, Chang CL, Chiu I, Cho HM, Clocchiatti A, Crawford TM, Crites AT, de Haan T, Desai S, Dobbs MA, Foley RJ, Forman WR, Garmire GP, George EM, Gladders MD, Gonzalez AH, Grandis S, Gupta N, Halverson NW, Hlavacek-Larrondo J, Hoekstra H, Holder GP, Holzapfel WL, Hou Z, Hrubes JD, Huang N, Jones C, Khullar G, Knox L, Kraft R, Lee AT, von der Linden A, Luong-Van D, Mantz A, Marrone DP, McDonald M, McMahon JJ, Meyer SS, Mocanu LM, Mohr JJ, Morris RG, Padin S, Patil S, Pryke C, Rapetti D, Reichardt CL, Rest A, Ruhl JE, Saliwanchik BR, Saro A, Sayre JT, Schaffer KK, Shirokoff E, Stalder B, Stanford SA, Staniszewski Z, Stark AA, Story KT, Strazzullo V, Stubbs CW, Vanderlinde K, Vieira JD, Vikhlinin A, Williamson R and Zenteno A (2019), Jun. Cluster Cosmology Constraints from the 2500 deg<sup>2</sup> SPT-SZ Survey: Inclusion of Weak Gravitational Lensing Data from Magellan and the Hubble Space Telescope. *Astrophys. J.* 878 (1), 55. doi:10.3847/1538-4357/ab1f10. [1812.01679](#).
- Boughn S and Crittenden R (2004), Jan. A correlation between the cosmic microwave background and large-scale structure in the Universe. *Nature* 427 (6969): 45–47. doi:10.1038/nature02139. [astro-ph/0305001](#).
- Calabrese M, Carbone C, Fabbian G, Baldi M and Baccigalupi C (2015), Mar. Multiple lensing of the cosmic microwave background anisotropies. *J. Cosmol. Astropart. Phys.* 2015 (3): 049–049. doi:10.1088/1475-7516/2015/03/049. [1409.7680](#).
- Calafut V, Gallardo P, Vavagiakis E, Amodeo S, Aiola S, Austermann J, Battaglia N, Battistelli E, Beall J, Bean R and et al. (2021), Aug. The atacama cosmology telescope: Detection of the pairwise kinematic sunyaev-zel'dovich effect with sdss dr15 galaxies. *Physical Review D* 104 (4). ISSN 2470-0029. doi:10.1103/physrevd.104.043502. <http://dx.doi.org/10.1103/PhysRevD.104.043502>.
- Carlstrom JE, Holder GP and Reese ED (2002). Cosmology with the Sunyaev-Zel'dovich Effect. *Annual Review of Astron and Astrophysics*. 40: 643–680.
- Carlstrom JE, Ade PAR, Aird KA, Benson BA, Bleem LE, Busetti S, Chang CL, Chauvin E, Cho HM, Crawford TM, Crites AT, Dobbs MA, Halverson NW, Heimsath S, Holzapfel WL, Hrubes JD, Joy M, Keisler R, Lanting TM, Lee AT, Leitch EM, Leong J, Lu W, Lueker M, Luong-Van D, McMahon JJ, Mehl J, Meyer SS, Mohr JJ, Montroy TE, Padin S, Plagge T, Pryke C, Ruhl JE, Schaffer KK, Schwan D, Shirokoff E, Spieler HG, Staniszewski Z, Stark AA, Tucker C, Vanderlinde K, Vieira JD and Williamson R (2011), May. The 10 Meter South Pole Telescope. *Publications of the ASP* 123 (903): 568. doi:10.1086/659879. [0907.4445](#).
- Caron J and Lewis A (2017), Sep. Maximum a posteriori cmb lensing reconstruction. *Physical Review D* 96 (6). ISSN 2470-0029. doi:10.1103/physrevd.96.063510. <http://dx.doi.org/10.1103/PhysRevD.96.063510>.
- Caron J, Mirmelstein M and Lewis A (2022), Sep. Cmb lensing from planck pr4 maps. *Journal of Cosmology and Astroparticle Physics* 2022 (09): 039. ISSN 1475-7516. doi:10.1088/1475-7516/2022/09/039. <http://dx.doi.org/10.1088/1475-7516/2022/09/039>.
- Challinor A and Lewis A (2005), May. Lensed CMB power spectra from all-sky correlation functions. *Phys. Rev. D* 71 (10): 103010–+. doi: 10.1103/PhysRevD.71.103010. [arXiv:astro-ph/0502425](#).



- doi:10.1103/PhysRevD.91.083533. 1401.1193.
- Ferraro S, Schaan E and Pierpaoli E (2022). Is the rees-sciama effect detectable by the next generation of cosmological experiments? 2205.10332, <https://arxiv.org/abs/2205.10332>.
- Fosalba P, Gaztañaga E and Castander FJ (2003), Nov. Detection of the Integrated Sachs-Wolfe and Sunyaev-Zeldovich Effects from the Cosmic Microwave Background-Galaxy Correlation. *Astrophys. J. Lett.* 597: L89–L92. doi:10.1086/379848. arXiv:astro-ph/0307249.
- Ge F, Millea M, Camphuis E, Daley C, Huang N, Omori Y, Quan W, Anderes E, Anderson AJ, Ansarinejad B, Archipley M, Balkenhol L, Benabed K, Bender AN, Benson BA, Bianchini F, Bleem LE, Bouchet FR, Bryant L, Carlstrom JE, Chang CL, Chaubal P, Chen G, Chichura PM, Chokshi A, Chou TL, Coerver A, Crawford TM, de Haan T, Dibert KR, Dobbs MA, Doohan M, Doussot A, Dutcher D, Everett W, Feng C, Ferguson KR, Fichman K, Foster A, Galli S, Gambrel AE, Gardner RW, Goeckner-Wald N, Gualtieri R, Guidi F, Guns S, Halverson NW, Hivon E, Holder GP, Holzapfel WL, Hood JC, Howe D, Hryciuk A, Kéruzoré F, Khalife AR, Knox L, Korman M, Kornelje K, Kuo CL, Lee AT, Levy K, Lowitz AE, Lu C, Maniyar A, Martsen ES, Menanteau F, Montgomery J, Nakato Y, Natoli T, Noble GI, Pan Z, Paschos P, Phadke KA, Pollak AW, Prabhu K, Rahimi M, Rahlin A, Reichardt CL, Riebel D, Rouble M, Ruhl JE, Schiappucci E, Sobrin JA, Stark AA, Stephen J, Tandoi C, Thorne B, Tredafilova C, Umita C, Vieira JD, Vitrier A, Wan Y, Whitehorn N, Wu WLK, Young MR and Zebrowski JA (2024). Cosmology from cmb lensing and delensed ee power spectra using 2019-2020 spt-3g polarization data 2411.06000, <https://arxiv.org/abs/2411.06000>.
- Geach JE and Peacock JA (2017). Cluster richness-mass calibration with cosmic microwave background lensing. *Nature Astron.* 1 (11): 795–799. doi:10.1038/s41550-017-0259-1. 1707.09369.
- Giani L, Howlett C, Ruggeri R, Bianchini F, Said K and Davis TM (2023). Cross-correlating radial peculiar velocities and CMB lensing convergence. *JCAP* 05: 002. doi:10.1088/1475-7516/2023/05/002. 2301.08381.
- Giannantonio T, Crittenden RG, Nichol RC, Scranton R, Richards GT, Myers AD, Brunner RJ, Gray AG, Connolly AJ and Schneider DP (2006), Sep. High redshift detection of the integrated sachs-wolfe effect. *Physical Review D* 74 (6). ISSN 1550-2368. doi:10.1103/physrevd.74.063520. <http://dx.doi.org/10.1103/PhysRevD.74.063520>.
- Granett BR, Neyrinck MC and Szapudi I (2008), Aug. An Imprint of Superstructures on the Microwave Background due to the Integrated Sachs-Wolfe Effect. *Astrophys. J. Lett.* 683 (2): L99. doi:10.1086/591670. 0805.3695.
- Hadzhiyska B, Ferraro S, Guachalla BR, Schaan E, Aguilar J, Battaglia N, Bond JR, Brooks D, Calabrese E, Choi SK, Claybaugh T, Coulton WR, Dawson K, Devlin M, Dey B, Doel P, Duivenvoorden AJ, Dunkley J, Farren GS, Font-Ribera A, Forero-Romero JE, Gallardo PA, Gaztañaga E, Gontcho SG, Gralla M, Guillou LL, Gutierrez G, Guy J, Hill JC, Hložek R, Honscheid K, Juneau S, Kisner T, Kremin A, Landriau M, Liu RH, Louis T, MacCrann N, de Macorra A, Madhavacheril M, Manera M, Meisner A, Miquel R, Moodley K, Moustakas J, Mroczkowski T, Naess S, Newman J, Niemack MD, Niz G, Page L, Palanque-Delabrouille N, Partridge B, Percival WJ, Prada F, Qu FJ, Rossi G, Sanchez E, Schlegel D, Schubnell M, Sehgal N, Seo H, Sifón C, Spergel D, Sprayberry D, Staggs S, Tarle G, Vargas C, Vavagiakis EM, Weaver BA, Wollack EJ, Zhou R and Zou H (2024). Evidence for large baryonic feedback at low and intermediate redshifts from kinematic sunyaev-zel'dovich observations with act and desi photometric galaxies 2407.07152, <https://arxiv.org/abs/2407.07152>.
- Hagstotz S, Schäfer BM and Merkel PM (2015), Nov. Born-corrections to weak lensing of the cosmic microwave background temperature and polarization anisotropies. *Mon. Not. R. Astron. Soc.* 454 (1): 831–838. doi:10.1093/mnras/stv1977. 1410.8452.
- Han D, Sehgal N and Villaescusa-Navarro F (2021), Dec. Deep learning simulations of the microwave sky. *Physical Review D* 104 (12). ISSN 2470-0029. doi:10.1103/physrevd.104.123521. <http://dx.doi.org/10.1103/PhysRevD.104.123521>.
- Hand N, Addison GE, Aubourg E, Battaglia N, Battistelli ES, Bizyaev D, Bond JR, Brewington H, Brinkmann J, Brown BR, Das S, Dawson KS, Devlin MJ, Dunkley J, Dunner R, Eisenstein DJ, Fowler JW, Gralla MB, Hajian A, Halpern M, Hilton M, Hincks AD, Hložek R, Hughes JP, Infante L, Irwin KD, Kosowsky A, Lin YT, Malanushenko E, Malanushenko V, Marriage TA, Marsden D, Menanteau F, Moodley K, Niemack MD, Nolta MR, Oravetz D, Page LA, Palanque-Delabrouille N, Pan K, Reese ED, Schlegel DJ, Schneider DP, Sehgal N, Shelden A, Sievers J, Sifón C, Simmons A, Snedden S, Spergel DN, Staggs ST, Swetz DS, Switzer ER, Trac H, Weaver BA, Wollack EJ, Yeh C and Zunckel C (2012), Jul. Evidence of Galaxy Cluster Motions with the Kinematic Sunyaev-Zel'dovich Effect. *Physical Review Letters* 109 (4), 041101. doi:10.1103/PhysRevLett.109.041101. 1203.4219.
- Hand N and et al. (2015). First Measurement of the Cross-Correlation of CMB Lensing and Galaxy Lensing. *Phys. Rev. D* 91 (6): 062001. doi:10.1103/PhysRevD.91.062001. 1311.6200.
- Hanson D, Challinor A and Lewis A (2010), Jun. Weak lensing of the cmb. *General Relativity and Gravitation* 42 (9): 2197–2218. ISSN 1572-9532. doi:10.1007/s10714-010-1036-y. <http://dx.doi.org/10.1007/s10714-010-1036-y>.
- Hanson D, Challinor A, Efstathiou G and Bielewicz P (2011), Feb. Cmb temperature lensing power reconstruction. *Physical Review D* 83 (4). ISSN 1550-2368. doi:10.1103/physrevd.83.043005. <http://dx.doi.org/10.1103/PhysRevD.83.043005>.
- Hasselfield M, Hilton M, Marriage TA, Addison GE, Barrientos LF, Battaglia N, Battistelli ES, Bond JR, Crichton D, Das S, Devlin MJ, Dicker SR, Dunkley J, Dünner R, Fowler JW, Gralla MB, Hajian A, Halpern M, Hincks AD, Hložek R, Hughes JP, Infante L, Irwin KD, Kosowsky A, Marsden D, Menanteau F, Moodley K, Niemack MD, Nolta MR, Page LA, Partridge B, Reese ED, Schmitt BL, Sehgal N, Sherwin BD, Sievers J, Sifón C, Spergel DN, Staggs ST, Swetz DS, Switzer ER, Thornton R, Trac H and Wollack EJ (2013), Jul. The atacama cosmology telescope: Sunyaev-zel'dovich selected galaxy clusters at 148 ghz from three seasons of data. *Journal of Cosmology and Astroparticle Physics* 2013 (07): 008–008. ISSN 1475-7516. doi:10.1088/1475-7516/2013/07/008. <http://dx.doi.org/10.1088/1475-7516/2013/07/008>.
- Henderson SW, Allison R, Austermann J, Baillod T, Battaglia N, Beall JA, Becker D, De Bernardis F, Bond JR, Calabrese E, Choi SK, Coughlin KP, Crowley KT, Datta R, Devlin MJ, Duff SM, Dunkley J, Dünner R, van Engelen A, Gallardo PA, Grace E, Hasselfield M, Hills F, Hilton GC, Hincks AD, Hložek R, Ho SP, Hubmayr J, Huffenberger K, Hughes JP, Irwin KD, Koopman BJ, Kosowsky AB, Li D, McMahon J, Munson C, Nati F, Newburgh L, Niemack MD, Niraula P, Page LA, Pappas CG, Salatino M, Schillaci A, Schmitt BL, Sehgal N, Sherwin BD, Sievers JL, Simon SM, Spergel DN, Staggs ST, Stevens JR, Thornton R, Van Lanen J, Vavagiakis EM, Ward JT and Wollack EJ (2016), Aug. Advanced ACTPol Cryogenic Detector Arrays and Readout. *Journal of Low Temperature Physics* 184: 772–779. doi:10.1007/s10909-016-1575-z. 1510.02809.
- Hill JC and Spergel DN (2014), Feb. Detection of thermal sz-cmb lensing cross-correlation in planck nominal mission data. *Journal of Cosmology and Astroparticle Physics* 2014 (02): 030–030. ISSN 1475-7516. doi:10.1088/1475-7516/2014/02/030. <http://dx.doi.org/10.1088/1475-7516/2014/02/030>.
- Hill JC, Ferraro S, Battaglia N, Liu J and Spergel DN (2016), Jul. Kinematic sunyaev-zel'dovich effect with projected fields: A novel probe of the baryon distribution with planck, wmap, and wise data. *Physical Review Letters* 117 (5). ISSN 1079-7114. doi:10.1103/physrevlett.117.051301. <http://dx.doi.org/10.1103/PhysRevLett.117.051301>.
- Hilton M and et al. (ACT, DES) (2021). The Atacama Cosmology Telescope: A Catalog of >4000 Sunyaev-Zel'dovich Galaxy Clusters. *Astrophys. J. Suppl.* 253 (1): 3. doi:10.3847/1538-4365/abd023. 2009.11043.
- Hirata CM and Seljak U (2003), Oct. Reconstruction of lensing from the cosmic microwave background polarization. *Phys. Rev. D* 68 (8): 083002–+. doi:10.1103/PhysRevD.68.083002. arXiv:astro-ph/0306354.
- Holder GP, Viero MP, Zahn O, Aird KA, Benson BA, Bhattacharya S, Bleem LE, Bock J, Brodin M, Carlstrom JE, Chang CL, Cho HM, Conley A, Crawford TM, Crites AT, de Haan T, Dobbs MA, Dudley J, George EM, Halverson NW, Holzapfel WL, Hoover S, Hou Z, Hrubes JD, Keisler R, Knox L, Lee AT, Leitch EM, Lueker M, Luong-Van D, Marsden G, Marrone DP, McMahon JJ, Mehl J, Meyer SS, Millea M, Mohr JJ, Montroy

- TE, Padin S, Plagge T, Pryke C, Reichardt CL, Ruhl JE, Sayre JT, Schaffer KK, Schulz B, Shaw L, Shirokoff E, Spieler HG, Staniszewski Z, Stark AA, Story KT, van Engelen A, Vanderlinde K, Vieira JD, Williamson R and Zemcov M (2013), Jul. A Cosmic Microwave Background Lensing Mass Map and Its Correlation with the Cosmic Infrared Background. *Astrophys. J. Lett.* 771, L16. doi:10.1088/2041-8205/771/1/L16. 1303.5048.
- Hotinli SC and Pierpaoli E (2024). On the detectability of the moving lens signal in cmb experiments. 2401.12280, <https://arxiv.org/abs/2401.12280>.
- Hotinli SC, Meyers J, Dalal N, Jaffe AH, Johnson MC, Mertens JB, Münchmeyer M, Smith KM and van Engelen A (2019), Aug. Transverse velocities with the moving lens effect. *Physical Review Letters* 123 (6). ISSN 1079-7114. doi:10.1103/physrevlett.123.061301. <http://dx.doi.org/10.1103/PhysRevLett.123.061301>.
- Hotinli SC, Smith KM, Madhavacheril MS and Kamionkowski M (2021), Oct. Cosmology with the moving lens effect. *Physical Review D* 104 (8). ISSN 2470-0029. doi:10.1103/physrevd.104.083529. <http://dx.doi.org/10.1103/PhysRevD.104.083529>.
- Hu W (2000). Weak lensing of the CMB: A harmonic approach. *Phys. Rev. D* 62: 043007. doi:10.1103/PhysRevD.62.043007. astro-ph/0001303.
- Hu W and Dodelson S (2002), Jan. Cosmic Microwave Background Anisotropies. *Annual Review of Astron and Astrophysics*. 40: 171–216. doi:10.1146/annurev.astro.40.060401.093926. astro-ph/0110414.
- Hu W and Okamoto T (2002). Mass Reconstruction with Cosmic Microwave Background Polarization. *The Astrophysical Journal* 574 (2): 566–574. ISSN 0004-637X. doi:10.1086/341110. 0111606.
- Huang N, Bleem LE, Stalder B, Ade PAR, Allen SW, Anderson AJ, Austermann JE, Avva JS, Beall JA, Bender AN, Benson BA, Bianchini F, Bocquet S, Brodin M, Carlstrom JE, Chang CL, Chiang HC, Citron R, Moran CC, Crawford TM, Crites AT, Haan Td, Dobbs MA, Everett W, Floyd B, Gallicchio J, George EM, Gilbert A, Gladders MD, Guns S, Gupta N, Halverson NW, Harrington N, Henning JW, Hilton GC, Holder GP, Holzapfel WL, Hrubes JD, Hubmayr J, Irwin KD, Khullar G, Knox L, Lee AT, Li D, Lowitz A, McDonald M, McMahon JJ, Meyer SS, Mocanu LM, Montgomery J, Nadolski A, Natoli T, Nibarger JP, Noble G, Novosad V, Padin S, Patil S, Pryke C, Reichardt CL, Ruhl JE, Saliwanchik BR, Saro A, Sayre JT, Schaffer KK, Sharon K, Sievers C, Smecher G, Stark AA, Story KT, Tucker C, Vanderlinde K, Veach T, Vieira JD, Wang G, Whitehorn N, Wu WLK and Yefremenko V (2020), Feb. Galaxy clusters selected via the sunyaev–zel'dovich effect in the sptpol 100-square-degree survey. *The Astronomical Journal* 159 (3): 110. ISSN 1538-3881. doi:10.3847/1538-3881/ab6a96. <http://dx.doi.org/10.3847/1538-3881/ab6a96>.
- Hurier G (2016), Dec. High significance detection of the tsz effect relativistic corrections. *Astronomy& Astrophysics* 596: A61. ISSN 1432-0746. doi:10.1051/0004-6361/201629726. <http://dx.doi.org/10.1051/0004-6361/201629726>.
- Ilić S, Langer M and Douspis M (2013), Jul. Detecting the integrated sachs-wolfe effect with stacked voids. *Astronomy& Astrophysics* 556: A51. ISSN 1432-0746. doi:10.1051/0004-6361/201321150. <http://dx.doi.org/10.1051/0004-6361/201321150>.
- Itoh N, Kohyama Y and Nozawa S (1998), Jul. Relativistic Corrections to the Sunyaev-Zeldovich Effect for Clusters of Galaxies. *Astrophys. J.* 502 (1): 7–15. doi:10.1086/305876. astro-ph/9712289.
- Knox L and Song Y (2002), Jul. Limit on the Detectability of the Energy Scale of Inflation. *Physical Review Letters* 89 (1): 011303–+. doi:10.1103/PhysRevLett.89.011303. arXiv:astro-ph/0202286.
- Komatsu E and et al. (WMAP) (2009). Five-Year Wilkinson Microwave Anisotropy Probe (WMAP) Observations: Cosmological Interpretation. *Astrophys. J. Suppl.* 180: 330–376. doi:10.1088/0067-0049/180/2/330. 0803.0547.
- Kovács A and et al. (DES) (2019). More out of less: an excess integrated Sachs-Wolfe signal from supervoids mapped out by the Dark Energy Survey. *Mon. Not. Roy. Astron. Soc.* 484: 5267–5277. doi:10.1093/mnras/stz341. 1811.07812.
- Krause E and Hirata CM (2010), Nov. Weak lensing power spectra for precision cosmology: Multiple-deflection, reduced shear, and lensing bias corrections. *Astronomy& Astrophysics* 523: A28. ISSN 1432-0746. doi:10.1051/0004-6361/200913524. <http://dx.doi.org/10.1051/0004-6361/200913524>.
- Krolewski A and Ferraro S (2022), Apr. The Integrated Sachs Wolfe effect: unWISE and Planck constraints on dynamical dark energy. *J. Cosmol. Astropart. Phys.* 2022 (4), 033. doi:10.1088/1475-7516/2022/04/033. 2110.13959.
- Krolewski A, Ferraro S, Schlafly EF and White M (2020), May. Unwise tomography of planck cmb lensing. *Journal of Cosmology and Astroparticle Physics* 2020 (05): 047–047. ISSN 1475-7516. doi:10.1088/1475-7516/2020/05/047. <http://dx.doi.org/10.1088/1475-7516/2020/05/047>.
- Kusiak A, Bolliet B, Ferraro S, Hill JC and Krolewski A (2021), Aug. Constraining the baryon abundance with the kinematic Sunyaev-Zel'dovich effect: Projected-field detection using P lanck , WMAP , and u n W I S E. *Phys. Rev. D* 104 (4), 043518. doi:10.1103/PhysRevD.104.043518. 2102.01068.
- Lewis A and Challinor A (2006). Weak gravitational lensing of the CMB. doi:10.1016/j.physrep.2006.03.002. 0601594.
- Lewis A and Challinor A (2006), Jun. Weak gravitational lensing of the CMB. *Phys. Rep.* 429: 1–65. doi:10.1016/j.physrep.2006.03.002. arXiv:astro-ph/0601594.
- Lewis A, Hall A and Challinor A (2017), Aug. Emission-angle and polarization-rotation effects in the lensed cmb. *Journal of Cosmology and Astroparticle Physics* 2017 (08): 023–023. ISSN 1475-7516. doi:10.1088/1475-7516/2017/08/023. <http://dx.doi.org/10.1088/1475-7516/2017/08/023>.
- Li C and Cooray A (2006), Jul. Weak lensing of the cosmic microwave background by foreground gravitational waves. *Physical Review D* 74 (2). ISSN 1550-2368. doi:10.1103/physrevd.74.023521. <http://dx.doi.org/10.1103/PhysRevD.74.023521>.
- Liu J and Hill JC (2015). Cross-correlation of Planck CMB Lensing and CFHTLenS Galaxy Weak Lensing Maps. *Phys. Rev. D* 92 (6): 063517. doi:10.1103/PhysRevD.92.063517. 1504.05598.
- Ma CP and Bertschinger E (1995), Dec. Cosmological perturbation theory in the synchronous and conformal newtonian gauges. *The Astrophysical Journal* 455: 7. ISSN 1538-4357. doi:10.1086/176550. <http://dx.doi.org/10.1086/176550>.
- Ma YZ and Zhao GB (2014). Dark energy imprints on the kinematic Sunyaev–Zel'dovich signal. *Phys. Lett. B* 735: 402–411. doi:10.1016/j.physletb.2014.06.066. 1309.1163.
- MacCrann N and et al. (2024). The Atacama Cosmology Telescope: reionization kSZ trispectrum methodology and limits. *Mon. Not. Roy. Astron. Soc.* 532 (4): 4247–4260. doi:10.1093/mnras/stac1746. 2405.01188.
- Madhavacheril M, Sehgal N, Allison R, Battaglia N, Bond JR, Calabrese E, Caliguri J, Coughlin K, Crichton D, Datta R, Devlin MJ, Dunkley J, Dünner R, Fogarty K, Grace E, Hajian A, Hasselfield M, Hill JC, Hilton M, Hincks AD, Hložek R, Hughes JP, Kosowsky A, Louis T, Lungu M, McMahon J, Moodley K, Munson C, Naess S, Nati F, Newburgh L, Niemack MD, Page LA, Partridge B, Schmitt B, Sherwin BD, Sievers J, Spergel DN, Staggs ST, Thornton R, Van Engelen A, Ward JT, Wollack EJ and Atacama Cosmology Telescope Collaboration (2015), Apr. Evidence of Lensing of the Cosmic Microwave Background by Dark Matter Halos. *Physical Review Letters* 114 (15), 151302. doi:10.1103/PhysRevLett.114.151302. 1411.7999.
- Madhavacheril MS, Hill JC, Naess S, Addison GE, Aiola S, Baildon T, Battaglia N, Bean R, Bond JR, Calabrese E, Calafut V, Choi SK, Darwisch O, Devlin MJ, Dunkley J, Dünner R, Ferraro S, Gallardo PA, Halpern M, Han D, Hasselfield M, Hilton M, Hincks AD, Hložek R, Ho SPP, Huffenberger KM, Hughes JP, Koopman BJ, Kosowsky A, Lokken M, Louis T, Lungu M, Maclnnis A, Maurin L, McMahon JJ, Moodley K, Nati F, Niemack MD, Page LA, Partridge B, Robertson N, Sehgal N, Schaan E, Schillaci A, Sherwin BD, Sifón C, Simon SM, Spergel DN, Staggs

- ST, Storer ER, van Engelen A, Vavagiakis EM, Wollack EJ and Xu Z (2019), Nov. The Atacama Cosmology Telescope: Component-separated maps of CMB temperature and the thermal Sunyaev-Zel'dovich effect. *arXiv e-prints*, arXiv:1911.05717v1911.05717.
- Madhavacheril MS, Qu FJ, Sherwin BD, MacCrann N, Li Y, Abril-Cabezas I, Ade PAR, Aiola S, Alford T, Amiri M, Amodeo S, An R, Atkins Z, Austermann JE, Battaglia N, Battistelli ES, Beall JA, Bean R, Beringue B, Bhadarkar T, Biermann E, Bolliet B, Bond JR, Cai H, Calabrese E, Calafut V, Capalbo V, Carrero F, Challinor A, Chesmore GE, Cho HM, Choi SK, Clark SE, Córdova Rosado R, Cothard NF, Coughlin K, Coulton W, Crowley KT, Dalal R, Darwish O, Devlin MJ, Dicker S, Doze P, Duell CJ, Duff SM, Duivenvoorden AJ, Dunkley J, Dünner R, Fanfani V, Fankhanel M, Farren G, Ferraro S, Freundt R, Fuzia B, Gallardo PA, Garrido X, Givans J, Gluscevic V, Golec JE, Guan Y, Hall KR, Halpern M, Han D, Harrison I, Hasselfield M, Healy E, Henderson S, Hensley B, Hervías-Caimapo C, Hill JC, Hilton GC, Hilton M, Hincks AD, Hložek R, Ho SPP, Huber ZB, Hubmayr J, Huffenberger KM, Hughes JP, Irwin K, Isopi G, Jense HT, Keller B, Kim J, Knowles K, Koopman BJ, Kosowsky A, Kramer D, Kusiak A, La Posta A, Lague A, Lakey V, Lee E, Li Z, Limon M, Lokken M, Louis T, Lungu M, Maclnnis A, Maldonado D, Maldonado F, Mallaby-Kay M, Marques GA, McMahon J, Mehta Y, Menanteau F, Moodley K, Morris TW, Mroczkowski T, Naess S, Namikawa T, Nati F, Newburgh L, Nicola A, Niemack MD, Nolta MR, Orlowski-Scherer J, Page LA, Pandey S, Partridge B, Prince H, Puddu R, Radiconi F, Robertson N, Rojas F, Sakuma T, Salatino M, Schaan E, Schmitt BL, Sehgal N, Shaikh S, Sierra C, Sievers J, Sifón C, Simon S, Sonka R, Spergel DN, Staggs ST, Storer E, Switzer ER, Tampier N, Thornton R, Trac H, Treu J, Tucker C, Ullom J, Vale LR, Van Engelen A, Van Lanen J, van Marrewijk J, Vargas C, Vavagiakis EM, Wagoner K, Wang Y, Wenzl L, Wollack EJ, Xu Z, Zago F and Zhang K (2023), Apr. The Atacama Cosmology Telescope: DR6 Gravitational Lensing Map and Cosmological Parameters. *arXiv e-prints*, arXiv:2304.05203doi:10.48550/arXiv.2304.05203. 2304.05203.
- Maniyar AS, Ali-Haïmoud Y, Carron J, Lewis A and Madhavacheril MS (2021), Apr. Quadratic estimators for cmb weak lensing. *Physical Review D* 103 (8). ISSN 2470-0029. doi:10.1103/physrevd.103.083524. <http://dx.doi.org/10.1103/PhysRevD.103.083524>.
- Marozzi G, Fanizza G, Di Dio E and Durrer R (2016), Sep. CMB-lensing beyond the Born approximation. *J. Cosmol. Astropart. Phys.* 2016 (9), 028. doi:10.1088/1475-7516/2016/09/028. 1605.08761.
- Marques GA and Bernui A (2020), Tomographic analyses of the CMB lensing and galaxy clustering to probe the linear structure growth. *JCAP* 05: 052. doi:10.1088/1475-7516/2020/05/052. 1908.04854.
- McCarthy F and Hill JC (2024), Cross-correlation of the thermal Sunyaev-Zel'dovich and CMB lensing signals in Planck PR4 data with robust CIB decontamination. *Phys. Rev. D* 109 (2): 023529. doi:10.1103/PhysRevD.109.023529. 2308.16260.
- McCarthy F, Battaglia N, Bean R, Bond JR, Cai H, Calabrese E, Coulton WR, Devlin MJ, Dunkley J, Ferraro S, Gluscevic V, Guan Y, Hill JC, Johnson MC, Kusiak A, Lagué A, MacCrann N, Madhavacheril MS, Moodley K, Naess S, Qu FJ, Guachalla BR, Sehgal N, Sherwin BD, Sifón C, Smith KM, Staggs ST, van Engelen A, Vavagiakis EM and Wollack EJ (2024), The atacama cosmology telescope: Large-scale velocity reconstruction with the kinematic sunyaev-zel'dovich effect and desi lrgs 2410.06229, <https://arxiv.org/abs/2410.06229>.
- McQuinn M, Furlanetto SR, Hernquist L, Zahn O and Zaldarriaga M (2005), Sep. The Kinetic Sunyaev-Zel'dovich Effect from Reionization. *Astrophys. J.* 630: 643–656. doi:10.1086/432049. astro-ph/0504189.
- Menanteau F, González J, Juin JB, Marriage TA, Reese ED, Acquaviva V, Aguirre P, Appel JW, Baker AJ, Barrientos LF, Battistelli ES, Bond JR, Das S, Deshpande AJ, Devlin MJ, Dicker S, Dunkley J, Dünner R, Essinger-Hileman T, Fowler JW, Hajian A, Halpern M, Hasselfeld M, Hernández-Monteagudo C, Hilton M, Hincks AD, Hložek R, Huffenberger KM, Hughes JP, Infante L, Irwin KD, Klein J, Kosowsky A, Lin YT, Marsden D, Moodley K, Niemack MD, Nolta MR, Page LA, Parker L, Partridge B, Sehgal N, Sievers J, Spergel DN, Staggs ST, Swetz D, Switzer E, Thornton R, Trac H, Warne R and Wollack E (2010), Oct. The atacama cosmology telescope: Physical properties and purity of a galaxy cluster sample selected via the sunyaev-zel'dovich effect. *The Astrophysical Journal* 723 (2): 1523–1541. ISSN 1538-4357. doi:10.1088/0004-637X/723/2/1523. <http://dx.doi.org/10.1088/0004-637X/723/2/1523>.
- Metcalf RB and Silk J (1997), Gravitational magnification of the cosmic microwave background. *Astrophys. J.* 489: 1–6. doi:10.1086/304756. astro-ph/9708059.
- Millea M and Seljak U (2022), May. Marginal unbiased score expansion and application to cmb lensing. *Physical Review D* 105 (10). ISSN 2470-0029. doi:10.1103/physrevd.105.103531. <http://dx.doi.org/10.1103/PhysRevD.105.103531>.
- Millea M, Anderes E and Wandelt BD (2020), Dec. Sampling-based inference of the primordial cmb and gravitational lensing. *Physical Review D* 102 (12). ISSN 2470-0029. doi:10.1103/physrevd.102.123542. <http://dx.doi.org/10.1103/PhysRevD.102.123542>.
- Mueller EM, de Bernardis F, Bean R and Niemack MD (2015), Constraints on gravity and dark energy from the pairwise kinematic Sunyaev-Zeldovich effect. *Astrophys. J.* 808 (1): 47. doi:10.1088/0004-637X/808/1/47. 1408.6248.
- Münchmeyer M, Madhavacheril MS, Ferraro S, Johnson MC and Smith KM (2019), Oct. Constraining local non-gaussianities with kinetic sunyaev-zel'dovich tomography. *Physical Review D* 100 (8). ISSN 2470-0029. doi:10.1103/physrevd.100.083508. <http://dx.doi.org/10.1103/PhysRevD.100.083508>.
- Namikawa T, Yamauchi D and Taruya A (2012), Jan. Full-sky lensing reconstruction of gradient and curl modes from CMB maps. *J. Cosmol. Astropart. Phys.* 1, 007. doi:10.1088/1475-7516/2012/01/007. 1110.1718.
- Namikawa T and et al. (POLARBEAR, HSC) (2019), Evidence for the Cross-correlation between Cosmic Microwave Background Polarization Lensing from POLARBEAR and Cosmic Shear from Subaru Hyper Suprime-Cam. *Astrophys. J.* 882: 62. doi:10.3847/1538-4357/ab3424. 1904.02116.
- Namikawa T, Roy A, Sherwin BD, Battaglia N and Spergel DN (2021), Sep. Constraining reionization with the first measurement of the cross-correlation between the CMB optical-depth fluctuations and the Compton y -map. *Phys. Rev. D* 104 (6), 063514. doi:10.1103/PhysRevD.104.063514. 2102.00975.
- Nicola A, Refregier A and Amara A (2016), Integrated approach to cosmology: Combining CMB, large-scale structure and weak lensing. *Phys. Rev. D* 94 (8): 083517. doi:10.1103/PhysRevD.94.083517. 1607.01014.
- Nishizawa AJ (2014), Jun. The integrated Sachs-Wolfe effect and the Rees-Sciama effect. *Progress of Theoretical and Experimental Physics* 2014 (6), 06B110. doi:10.1093/ptep/ptu062. 1404.5102.
- Nishizawa AJ, Komatsu E, Yoshida N, Takahashi R and Sugiyama N (2008), Mar. Cosmic microwave background-weak lensing correlation: Analytical and numerical study of nonlinearity and implications for dark energy. *The Astrophysical Journal* 676 (2): L93–L96. ISSN 1538-4357. doi:10.1086/587741. <http://dx.doi.org/10.1086/587741>.
- Omori Y (2024), Jun. AGORA: Multicomponent simulation for cross-survey science. *Mon. Not. R. Astron. Soc.* 530 (4): 5030–5068. doi:10.1093/mnras/stae1031. 2212.07420.
- Omori Y, Chown R, Simard G, Story KT, Aylor K, Baxter EJ, Benson BA, Bleem LE, Carlstrom JE, Chang CL, Cho HM, Crawford TM, Crites AT, de Haan T, Dobbs MA, Everett WB, George EM, Halverson NW, Harrington NL, Holder GP, Hou Z, Holzapfel WL, Hruubes JD, Knox L, Lee AT, Leitch EM, Luong-Van D, Manzotti A, Marrone DP, McMahon JJ, Meyer SS, Mocanu LM, Mohr JJ, Natoli T, Padin S, Pryke C, Reichardt CL, Ruhl JE, Sayre JT, Schaffer KK, Shirokoff E, Staniszewski Z, Stark AA, Vanderlinde K, Vieira JD, Williamson R and Zahn O (2017), Nov. A 2500 deg<sup>2</sup> CMB Lensing Map from Combined South Pole Telescope and Planck Data. *Astrophys. J.* 849, 124. doi:10.3847/1538-4357/aa8d1d. 1705.00743.
- Omori Y and et al. (DES, SPT) (2019), Dark Energy Survey Year 1 Results: Tomographic cross-correlations between Dark Energy Survey

- galaxies and CMB lensing from South Pole Telescope+Planck. *Phys. Rev. D* 100 (4): 043501. doi:10.1103/PhysRevD.100.043501. 1810.02342.
- Pan Z, Knox L and White M (2014), Dec. Dependence of the cosmic microwave background lensing power spectrum on the matter density. *Mon. Not. R. Astron. Soc.* 445 (3): 2941–2945. doi:10.1093/mnras/stu1971. 1406.5459.
- Pan Z, Bianchini F, Wu W, Ade P, Ahmed Z, Anderson E, Anderson A, Ansarinejad B, Archipley M, Aylor K, Balkenhol L, Barry P, Basu Thakur R, Benabed K, Bender A, Benson B, Bleem L, Bouchet F, Bryant L, Byrum K, Camphuis E, Carlstrom J, Carter F, Cecil T, Chang C, Chabal P, Chen G, Chichura P, Cho HM, Chou TL, Cliche JF, Coerver A, Crawford T, Cukierman A, Daley C, de Haan T, Denison E, Dibert K, Ding J, Dobbs M, Doussot A, Dutcher D, Everett W, Feng C, Ferguson K, Fichman K, Foster A, Fu J, Galli S, Gambrel A, Gardner R, Ge F, Goeckner-Wald N, Gualtieri R, Guidi F, Guns S, Gupta N, Halverson N, Harke-Hosemann A, Harrington N, Henning J, Hilton G, Hivon E, Holder G, Holzapfel W, Hood J, Howe D, Huang N, Irwin K, Jeong O, Jonas M, Jones A, Kéruzoré F, Khaire T, Knox L, Kofman A, Korman M, Kubik D, Kuhlmann S, Kuo CL, Lee A, Leitch E, Levy K, Lowitz A, Lu C, Maniyar A, Menanteau F, Meyer S, Michalik D, Millea M, Montgomery J, Nadolski A, Nakato Y, Natoli T, Nguyen H, Noble G, Novosad V, Omori Y, Padin S, Paschos P, Pearson J, Posada C, Prabhu K, Quan W, Raghunathan S, Rahimi M, Rahlin A, Reichardt C, Riebel D, Riedel B, Ruhl J, Sayre J, Schiappucci E, Shirokoff E, Smecher G, Sobrin J, Stark A, Stephen J, Story K, Suzuki A, Takakura S, Tandoi C, Thompson K, Thorne B, Trendafilova C, Tucker C, Umita C, Vale L, Vanderlinde K, Vieira J, Wang G, Whitehorn N, Yefremenko V, Yoon K, Young M and Zebrowski J (2023), Dec. Measurement of gravitational lensing of the cosmic microwave background using spt-3g 2018 data. *Physical Review D* 108 (12). ISSN 2470-0029. doi:10.1103/physrevd.108.122005. <http://dx.doi.org/10.1103/PhysRevD.108.122005>.
- Park H, Shapiro PR, Komatsu E, Iliev IT, Ahn K and Mellema G (2013), May. The kinetic sunyaev-zel'dovich effect as a probe of the physics of cosmic reionization: The effect of self-reionizing reionization. *The Astrophysical Journal* 769 (2): 93. ISSN 1538-4357. doi:10.1088/0004-637x/769/2/93. <http://dx.doi.org/10.1088/0004-637x/769/2/93>.
- Peacock JA and Bilicki M (2018), Aug. Wide-area tomography of cmb lensing and the growth of cosmological density fluctuations. *Monthly Notices of the Royal Astronomical Society* 481 (1): 1133–1148. ISSN 1365-2966. doi:10.1093/mnras/sty2314. <http://dx.doi.org/10.1093/mnras/sty2314>.
- Peebles PJE and Yu JT (1970), Dec. Primeval adiabatic perturbation in an expanding universe. *Astrophys. J.* 162: 815.
- Planck Collaboration, Ade PAR, Aghanim N, Armitage-Caplan C, Arnaud M, Ashdown M, Atrio-Barandela F, Aumont J, Baccigalupi C, Banday AJ and et al. (2014a), Nov. Planck 2013 results. XVII. Gravitational lensing by large-scale structure. *Astron. Astrophys.* 571, A17. doi:10.1051/0004-6361/201321543. 1303.5077.
- Planck Collaboration, Ade PAR, Aghanim N, Armitage-Caplan C, Arnaud M, Ashdown M, Atrio-Barandela F, Aumont J, Baccigalupi C, Banday AJ and et al. (2014b), Nov. Planck 2013 results. XVIII. The gravitational lensing-infrared background correlation. *Astron. Astrophys.* 571, A18. doi:10.1051/0004-6361/201321540. 1303.5078.
- Planck Collaboration, Ade PAR, Aghanim N, Arnaud M, Ashdown M, Aumont J, Baccigalupi C, Banday AJ, Barreiro RB, Bartlett JG and et al. (2016a), Sep. Planck 2015 results. XV. Gravitational lensing. *Astron. Astrophys.* 594, A15. doi:10.1051/0004-6361/201525941. 1502.01591.
- Planck Collaboration, Ade PAR, Aghanim N, Arnaud M, Ashdown M, Aumont J, Baccigalupi C, Banday AJ, Barreiro RB, Bartlett JG and et al. (2016b), Sep. Planck 2015 results. XXIV. Cosmology from Sunyaev-Zeldovich cluster counts. *Astron. Astrophys.* 594, A24. doi:10.1051/0004-6361/201525833. 1502.01597.
- Planck Collaboration, Ade PAR, Aghanim N, Arnaud M, Ashdown M, Aumont J, Baccigalupi C, Banday AJ, Barreiro RB, Barrena R, Bartlett JG, Bartolo N, Battaner E, Battye R, Benabed K, Benoît A, Benoît-Lévy A, Bernard JP, Bersanelli M, Bielewicz P, Bikmaev I, Böhringer H, Bonaldi A, Bonavera L, Bond JR, Borrill J, Bouchet FR, Bucher M, Burenin R, Burigana C, Butler RC, Calabrese E, Cardoso JF, Carvalho P, Catalano A, Challinor A, Chamballu A, Chary RR, Chiang HC, Chon G, Christensen PR, Clements DL, Colombo S, Colombo LPL, Combet C, Comis B, Couchot F, Coulaas A, Crill BP, Curto A, Cuttaia F, Dahle H, Danese L, Davies RD, Davis RJ, de Bernardis P, de Rosa A, de Zotti G, Delabrouille J, Désert FX, Dickinson C, Diego JM, Dolag K, Dole H, Donzelli S, Doré O, Douspis M, Ducout A, Dupac X, Efstathiou G, Eisenhardt PRM, Elsner F, Enßlin TA, Eriksen HK, Falgarone E, Fergusson J, Feroz F, Ferragamo A, Finelli F, Forni O, Frailis M, Fraisse AA, Franceschi E, Frejsel A, Galeotta S, Galli S, Ganga K, Génova-Santos RT, Giard M, Giraud-Héraud Y, Gjerløw E, González-Nuevo J, Górska KM, Grainge KJB, Gratton S, Gregorio A, Gruppuso A, Gudmundsson JE, Hansen FK, Hanson D, Harrison DL, Hempel A, Henrot-Versillé S, Hernández-Monteagudo C, Herranz D, Hildebrandt SR, Hivon E, Hobson M, Holmes WA, Hornstrup A, Hovest W, Huffenberger KM, Hurier G, Jaffe AH, Jaffe TR, Jin T, Jones WC, Juvela M, Keihänen E, Keskitalo R, Khamitov I, Kisner TS, Kneissl R, Knoche J, Kunz M, Kurki-Suonio H, Lagache G, Lamarre JM, Lasenby A, Lattanzi M, Lawrence CR, Leonardi R, Lesgourgues J, Levrier F, Liguori M, Lilje PB, Linden-Vørnle M, López-Caniego M, Lubin PM, Macías-Pérez JF, Maggio G, Maino D, Mak DSY, Mandolesi N, Mangilli A, Martin PG, Martínez-González E, Masi S, Matarrese S, Mazzotta P, McGeehee P, Mei S, Melchiorri A, Melin JB, Mendes L, Mennella A, Migliaccio M, Mitra S, Miville-Deschénes MA, Moneti A, Montier L, Morgante G, Mortlock D, Moss A, Munshi D, Murphy JA, Naselsky P, Nastasi A, Nati F, Natoli P, Netterfield CB, Nørgaard-Nielsen HU, Noviello F, Novikov D, Novikov I, Olamaie M, Oxborrow CA, Paci F, Pagano L, Pajot F, Paoletti D, Pasian F, Patanchon G, Pearson TJ, Perdereau O, Perotto L, Perrott YC, Perrotta F, Pettorino V, Piacentini F, Piat M, Pierpaoli E, Pietrobon D, Plaszczynski S, Pointecouteau E, Polenta G, Pratt GW, Prézeau G, Prunet S, Puget JL, Rachen JP, Reach WT, Rebolo R, Reinecke M, Remazeilles M, Renault C, Renzi A, Ristorcelli I, Rocha G, Rossetti M, Roudier G, Rozo E, Rubiño-Martín JA, Rumsey C, Rusholme B, Rykoff ES, Sandri M, Santos D, Saunders RDE, Savelainen M, Savini G, Schammel MP, Scott D, Seiffert MD, Shellard EPS, Shimwell TW, Spencer LD, Stanford SA, Stern D, Stolyarov V, Stompor R, Streblyanska A, Sudivala R, Sunyaev R, Sutton D, Suur-Uski AS, Sygnet JF, Tauber JA, Terenzi L, Toffolatti L, Tomasi M, Tramonte D, Tristram M, Tucci M, Tuovinen J, Umana G, Valenziano L, Valiviita J, Van Tent B, Vielva P, Villa F, Wade LA, Wandelt BD, Wehus IK, White SDM, Wright EL, Yvon D, Zacchei A and Zonca A (2016c), Sep. Planck 2015 results. XXVII. The second Planck catalogue of Sunyaev-Zeldovich sources. *Astron. Astrophys.* 594, A27. doi:10.1051/0004-6361/201525823. 1502.01598.
- Planck Collaboration, Aghanim N, Arnaud M, Ashdown M, Aumont J, Baccigalupi C, Banday AJ, Barreiro RB, Bartlett JG, Bartolo N, Battaner E, Battye R, Benabed K, Benoît A, Benoît-Lévy A, Bernard JP, Bersanelli M, Bielewicz P, Bock JJ, Bonaldi A, Bonavera L, Bond JR, Borrill J, Bouchet FR, Burigana C, Butler RC, Calabrese E, Cardoso JF, Catalano A, Challinor A, Chiang HC, Christensen PR, Churazov E, Clements DL, Colombo LPL, Combet C, Comis B, Coulaas A, Crill BP, Curto A, Cuttaia F, Danese L, Davies RD, Davis RJ, de Bernardis P, de Rosa A, de Zotti G, Delabrouille J, Désert FX, Dickinson C, Diego JM, Dolag K, Dole H, Donzelli S, Doré O, Douspis M, Ducout A, Dupac X, Efstathiou G, Elsner F, Enßlin TA, Eriksen HK, Fergusson J, Finelli F, Forni O, Frailis M, Fraisse AA, Franceschi E, Frejsel A, Galeotta S, Galli S, Ganga K, Génova-Santos RT, Giard M, González-Nuevo J, Górska KM, Gregorio A, Gruppuso A, Gudmundsson JE, Hansen FK, Harrison DL, Henrot-Versillé S, Hernández-Monteagudo C, Herranz D, Hildebrandt SR, Hivon E, Holmes WA, Hornstrup A, Huffenberger KM, Hurier G, Jaffe AH, Jones WC, Juvela M, Keihänen E, Keskitalo R, Kneissl R, Knoche J, Kunz M, Kurki-Suonio H, Lacasa F, Lagache G, Lähteenmäki A, Lamarre JM, Lasenby A, Lattanzi M, Leonardi R, Lesgourgues J, Levrier F, Liguori M, Lilje PB, Linden-Vørnle M, López-Caniego M, Macías-Pérez JF, Maffei B, Maggio G, Maino D, Mandolesi N, Mangilli A, Maris M, Martin PG, Martínez-González E, Masi S, Matarrese S, Melchiorri A, Melin JB, Migliaccio M, Miville-Deschénes MA, Moneti A, Montier L, Morgante G, Mortlock D, Munshi D, Murphy JA, Naselsky P, Nati F, Natoli P, Noviello F, Novikov D, Novikov I, Paci F, Pagano L, Pajot F, Paoletti D, Pasian F, Patanchon G, Perdereau O, Perotto L, Pettorino V, Piacentini F, Piat M, Pierpaoli E, Pietrobon D, Plaszczynski S, Pointecouteau E, Polenta G, Ponthieu N, Pratt GW, Prunet S, Puget JL, Rachen JP, Reinecke M, Remazeilles M, Renault C, Renzi A, Ristorcelli I, Rocha G, Rossetti M, Roudier G, Rubiño-Martín JA, Rusholme B, Sandri M,

- Santos D, Sauvé A, Savelainen M, Savini G, Scott D, Spencer LD, Stolyarov V, Stompor R, Sunyaev R, Sutton D, Suur-Uski AS, Sygnet JF, Tauber JA, Terenzi L, Toffolatti L, Tomasi M, Tramonte D, Tristram M, Tucci M, Tuovinen J, Valenziano L, Valiviita J, Van Tent B, Vielva P, Villa F, Wade LA, Wandelt BD, Wehus IK, Yvon D, Zacchei A and Zonca A (2016d), Sep. Planck 2015 results. XXII. A map of the thermal Sunyaev-Zeldovich effect. *Astron. Astrophys.* 594, A22. doi:10.1051/0004-6361/201525826. 1502.01596.
- Planck Collaboration, Aghanim N, Akrami Y, Ashdown M, Aumont J, Baccigalupi C, Ballardini M, Banday AJ, Barreiro RB, Bartolo N, Basak S, Battye R, Benabed K, Bernard JP, Bersanelli M, Bielewicz P, Bock JJ, Bond JR, Borrill J, Bouchet FR, Boulanger F, Bucher M, Burigana C, Butler RC, Calabrese E, Cardoso JF, Carron J, Challinor A, Chiang HC, Chluba J, Colombo LPL, Combet C, Contreras D, Crill BP, Cuttaia F, de Bernardis P, de Zotti G, Delabrouille J, Delouis JM, Di Valentino E, Diego JM, Doré O, Douspis M, Ducout A, Dupac X, Dusini S, Efstatius G, Elsner F, EnBlin TA, Eriksen HK, Fantaye Y, Farhang M, Fergusson J, Fernandez-Cobos R, Finelli F, Forastieri F, Frailis M, Fraisse AA, Franceschi E, Frolov A, Galeotta S, Galli S, Ganga K, Génova-Santos RT, Gerbino M, Ghosh T, González-Nuevo J, Górski KM, Gratton S, Gruppuso A, Gudmundsson JE, Hamann J, Handley W, Hansen FK, Herranz D, Hildebrandt SR, Hivon E, Huang Z, Jaffe AH, Jones WC, Karakci A, Keihänen E, Keskitalo R, Kiiveri K, Kim J, Kisner TS, Knox L, Krachmalnicoff N, Kunz M, Kurki-Suonio H, Lagache G, Lamarre JM, Lasenby A, Lattanzi M, Lawrence CR, Le Jeune M, Lemos P, Lesgourgues J, Levrier F, Lewis A, Liguori M, Lilje PB, Lilley M, Lindholm V, López-Caniego M, Lubin PM, Ma YZ, Macías-Pérez JF, Maggio G, Maino D, Mandolesi N, Mangilli A, Marcos-Caballero A, Maris M, Martin PG, Martinelli M, Martínez-González E, Matarrese S, Mauri N, McEwen JD, Meinhold PR, Melchiorri A, Mennella A, Migliaccio M, Millea M, Mitra S, Miville-Deschénes MA, Molinari D, Montier L, Morgante G, Moss A, Natoli P, Nørgaard-Nielsen HU, Pagano L, Paoletti D, Partridge B, Patanchon G, Peiris HV, Perrotta F, Pettorino V, Piacentini F, Polastri L, Polenta G, Puget JL, Rachen JP, Reinecke M, Remazeilles M, Renzi A, Rocha G, Rosset C, Roudier G, Rubiño-Martín JA, Ruiz-Granados B, Salvati L, Sandri M, Savelainen M, Scott D, Shellard EPS, Sirignano C, Sirri G, Spencer LD, Sunyaev R, Suur-Uski AS, Tauber JA, Tavagnacco D, Tenti M, Toffolatti L, Tomasi M, Trombetti T, Valenziano L, Valiviita J, Van Tent B, Vibert L, Vielva P, Villa F, Vittorio N, Wandelt BD, Wehus IK, Zacchei A and Zonca A (2020a), Sep. Planck 2018 results. VI. Cosmological parameters. *Astron. Astrophys.* 641, A6. doi:10.1051/0004-6361/201833910. 1807.06209.
- Planck Collaboration, Akrami Y, Andersen KJ, Ashdown M, Baccigalupi C, Ballardini M, Banday AJ, Barreiro RB, Bartolo N, Basak S, Benabed K, Bernard JP, Bersanelli M, Bielewicz P, Bond JR, Borrill J, Burigana C, Butler RC, Calabrese E, Casaponsa B, Chiang HC, Colombo LPL, Combet C, Crill BP, Cuttaia F, de Bernardis P, de Rosa A, de Zotti G, Delabrouille J, Di Valentino E, Diego JM, Doré O, Douspis M, Dupac X, Eriksen HK, Fernandez-Cobos R, Finelli F, Frailis M, Fraisse AA, Franceschi E, Frolov A, Galeotta S, Galli S, Ganga K, Gerbino M, Ghosh T, González-Nuevo J, Górski KM, Gruppuso A, Gudmundsson JE, Handley W, Helou G, Herranz D, Hildebrandt SR, Hivon E, Huang Z, Jaffe AH, Jones WC, Keihänen E, Keskitalo R, Kiiveri K, Kim J, Kisner TS, Krachmalnicoff N, Kunz M, Kurki-Suonio H, Lasenby A, Lattanzi M, Lawrence CR, Le Jeune M, Levrier F, Liguori M, Lilje PB, Lilley M, Lindholm V, López-Caniego M, Lubin PM, Macías-Pérez JF, Maino D, Mandolesi N, Marcos-Caballero A, Maris M, Martin PG, Martínez-González E, Matarrese S, Mauri N, McEwen JD, Meinhold PR, Mennella A, Migliaccio M, Mitra S, Molinari D, Montier L, Morgante G, Moss A, Natoli P, Paoletti D, Partridge B, Patanchon G, Pearson D, Pearson TJ, Perrotta F, Piacentini F, Polenta G, Rachen JP, Reinecke M, Remazeilles M, Renzi A, Rocha G, Rosset C, Roudier G, Rubiño-Martín JA, Ruiz-Granados B, Salvati L, Savelainen M, Scott D, Sirignano C, Sirri G, Spencer LD, Suur-Uski AS, Svalheim LT, Tauber JA, Tavagnacco D, Tenti M, Terenzi L, Thommesen H, Toffolatti L, Tomasi M, Trombetti T, Valiviita J, Van Tent B, Vielva P, Villa F, Vittorio N, Wandelt BD, Wehus IK, Zacchei A and Zonca A (2020b), Nov. Planck intermediate results. LVII. Joint Planck LFI and HFI data processing. *Astron. Astrophys.* 643, A42. doi:10.1051/0004-6361/202038073. 2007.04997.
- Pratten G and Lewis A (2016), Aug. Impact of post-born lensing on the cmb. *Journal of Cosmology and Astroparticle Physics* 2016 (08): 047–047. ISSN 1475-7516. doi:10.1088/1475-7516/2016/08/047. <http://dx.doi.org/10.1088/1475-7516/2016/08/047>.
- Qu FJ, Sherwin BD, Madhavaricheril MS, Han D, Crowley KT, Abril-Cabezas I, Ade PAR, Aiola S, Alford T, Amiri M, Amodeo S, An R, Atkins Z, Austermann JE, Battaglia N, Battistelli ES, Beall JA, Bean R, Beringue B, Bhandarkar T, Biermann E, Boller B, Bond JR, Cai H, Calabrese E, Calafut V, Capalbo V, Carrero F, Carron J, Challinor A, Cheshire GE, Cho HM, Choi SK, Clark SE, Córdoba Rosado R, Cothard NF, Coughlin K, Coulton W, Dalal R, Darwishi O, Devlin MJ, Dicker S, Doze P, Duell CJ, Duff SM, Duivenvoorden AJ, Dunkley J, Dünner R, Fanfani V, Fankhanel M, Farren G, Ferraro S, Freudent R, Fuzia B, Gallardo PA, Garrido X, Gluscevic V, Golec JE, Guan Y, Halpern M, Harrison I, Hasselfield M, Healy E, Henderson S, Hensley B, Hervás-Caimapo C, Hill JC, Hilton GC, Hilton M, Hincks AD, Hložek R, Ho SPP, Huber ZB, Hubmayr J, Huffenberger KM, Hughes JP, Irwin K, Isopi G, Jense HT, Keller B, Kim J, Knowles K, Koopman BJ, Kosowsky A, Kramer D, Kusiak A, La Posta A, Lague A, Lakey V, Lee E, Li Z, Li Y, Limon M, Lokken M, Louis T, Lungu M, MacCrann N, MacInnis A, Maldonado D, Maldonado F, Mallaby-Kay M, Marques GA, McMahon J, Mehta Y, Menanteau F, Moodley K, Morris TW, Mroczkowski T, Naess S, Namikawa T, Nati F, Newburgh L, Nicola A, Niemann MD, Nolta MR, Orlowski-Scherer J, Page LA, Pandey S, Partridge B, Prince H, Puddu R, Radiconi F, Robertson N, Rojas F, Sakuma T, Salatino M, Schaan E, Schmitt BL, Sehgal N, Shaikh S, Sierra C, Sievers J, Sifón C, Simon S, Sonka R, Spergel DN, Staggs ST, Storer E, Switzer ER, Tampier N, Thornton R, Trac H, Treu J, Tucker C, Ullom J, Vale LR, Van Engelen A, Van Lanen J, van Marrewijk J, Vargas C, Vavagiakis EM, Wagoner K, Wang Y, Wenzl L, Wollack EJ, Xu Z, Zago F and Zhang K (2023), Apr. The Atacama Cosmology Telescope: A Measurement of the DR6 CMB Lensing Power Spectrum and its Implications for Structure Growth. *arXiv e-prints*, arXiv:2304.05202doi:10.48550/arXiv.2304.05202. 2304.05202.
- Raghunathan S, Bianchini F and Reichardt CL (2018), Aug. Imprints of gravitational lensing in the Planck cosmic microwave background data at the location of WISE xSCOS galaxies. *Phys. Rev. D* 98 (4), 043506. doi:10.1103/PhysRevD.98.043506. 1710.09770.
- Raghunathan S, Patil S, Baxter E, Benson BA, Bleem LE, Chou TL, Crawford TM, Holder GP, McClintock T, Reichardt CL, Rozo E, Varga TN, Abbott TMC, Ade PAR, Allam S, Anderson AJ, Annis J, Austermann JE, Avila S, Beall JA, Bechtol K, Bender AN, Bernstein G, Bertin E, Bianchini F, Brooks D, Burke DL, Carlstrom JE, Carretero J, Chang CL, Chiang HC, Cho HM, Citron R, Crites AT, da Costa LN, Davis C, Desai S, Diehl HT, Dietrich JP, Dobbs MA, Doel P, Eifler TF, Everett W, Evrard AE, Flaugher B, Fosalba P, Frieman J, Gallicchio J, García-Bellido J, Gaztanaga E, George EM, Gilbert A, Gruen D, Gruendl RA, Gschwend J, Gupta N, Gutierrez G, de Haan T, Halverson NW, Harrington N, Hartley WG, Henning JW, Hilton GC, Hollowood DL, Holzapfel WL, Honscheid K, Hou Z, Hoyle B, Hrubes JD, Huang N, Hubmayr J, Irwin KD, James DJ, Jeltema T, Kim AG, Carrasco Kind M, Knox L, Kovacs A, Kuehn K, Kuropatkin N, Lee AT, Li TS, Lima M, Maia MAG, Marshall JL, McMahon JJ, Melchior P, Menanteau F, Meyer SS, Miller CJ, Miquel R, Mocanu L, Montgomery J, Nadolski A, Natoli T, Nibarger JP, Novosad V, Padin S, Plazaas AA, Pryke C, Rapetti D, Romer AK, Carnero Rosell A, Ruhl JE, Saliwanchik BR, Sanchez E, Sayre JT, Scarpine V, Schaffer KK, Schubnell M, Serrano S, Sevilla-Noarbe I, Smecher G, Smith RC, Soares-Santos M, Sobreira F, Stark AA, Story KT, Suchyta E, Swanson MEC, Tarle G, Thomas D, Tucker C, Vanderlinde K, De Vicente J, Vieira JD, Wang G, Whitehorn N, Wu WLK and Zhang Y (2019a), Feb. Mass Calibration of Optically Selected DES Clusters Using a Measurement of CMB-cluster Lensing with SPTpol Data. *Astrophys. J.* 872, 170. doi:10.3847/1538-4357/ab01ca. 1810.10998.
- Raghunathan S, Patil S, Baxter E, Benson BA, Bleem LE, Crawford TM, Holder GP, McClintock T, Reichardt CL, Varga TN, Whitehorn N, Ade PAR, Allam S, Anderson AJ, Austermann JE, Avila S, Avva JS, Bacon D, Beall JA, Bender AN, Bianchini F, Bocquet S, Brooks D, Burke DL, Carlstrom JE, Carretero J, Castander FJ, Chang CL, Chiang HC, Citron R, Costanzi M, Crites AT, da Costa LN, Desai S, Diehl HT, Dietrich JP, Dobbs MA, Doel P, Everett S, Evrard AE, Feng C, Flaugher B, Fosalba P, Frieman J, Gallicchio J, García-Bellido J, Gaztanaga E, George EM, Giannantonio T, Gilbert A, Gruendl RA, Gschwend J, Gupta N, Gutierrez G, de Haan T, Halverson NW, Harrington N, Henning JW, Hilton GC, Hollowood DL, Holzapfel WL, Honscheid K, Hrubes JD, Huang N, Hubmayr J, Irwin KD, Jeltema T, Carrasco Kind M, Knox L, Kuropatkin

- N, Lahav O, Lee AT, Li D, Lima M, Lowitz A, Maia MAG, Marshall JL, McMahon JJ, Melchior P, Menanteau F, Meyer SS, Miquel R, Mocanu LM, Mohr JJ, Montgomery J, Corbett Moran C, Nadolski A, Natoli T, Nibarger JP, Noble G, Novosad V, Ogando RLC, Padin S, Plazas AA, Pryke C, Rapetti D, Romer AK, Roodman A, Carnero Rosell A, Rozo E, Ruhl JE, Rykoff ES, Saliwanchik BR, Sanchez E, Sayre JT, Scarpine V, Schaffer KK, Schubnell M, Serrano S, Sevilla-Noarbe I, Sievers C, Smecher G, Smith M, Soares-Santos M, Stark AA, Story KT, Suchyta E, Swanson MEC, Tarle G, Tucker C, Vanderlinde K, Veach T, De Vicente J, Vieira JD, Vikram V, Wang G, Wu WLK, Yefremenko V and Zhang Y (2019b), Jul. A Detection of CMB-Cluster Lensing using Polarization Data from SPTpol. *arXiv e-prints*, arXiv:1907.08605.
- Raghunathan S, Whitehorn N, Alvarez MA, Aung H, Battaglia N, Holder GP, Nagai D, Pierpaoli E, Reichardt CL and Vieira JD (2022), Feb. Constraining cluster virialization mechanism and cosmology using thermal-sz-selected clusters from future cmb surveys. *The Astrophysical Journal* 926 (2): 172. ISSN 1538-4357. doi:10.3847/1538-4357/ac4712. <http://dx.doi.org/10.3847/1538-4357/ac4712>.
- Raghunathan S and et al. (SPT-3G, SPTpol) (2024). First Constraints on the Epoch of Reionization Using the Non-Gaussianity of the Kinematic Sunyaev-Zel'dovich Effect from the South Pole Telescope and Herschel-SPIRE Observations. *Phys. Rev. Lett.* 133 (12): 121004. doi:10.1103/PhysRevLett.133.121004. 2403.02337.
- Rees MJ and Scrimgeour DW (1968). Large scale Density Inhomogeneities in the Universe. *Nature* 217: 511–516. doi:10.1038/217511a0.
- Reichardt CL, Stalder B, Bleem LE, Montroy TE, Aird KA, Andersson K, Armstrong R, Ashby MLN, Bautz M, Bayliss M, Bazin G, Benson BA, Brodwin M, Carlstrom JE, Chang CL, Cho HM, Clocchiatti A, Crawford TM, Crites AT, de Haan T, Desai S, Dobbs MA, Dudley JP, Foley RJ, Forman WR, George EM, Gladders MD, Gonzalez AH, Halverson NW, Harrington NL, High FW, Holder GP, Holzapfel WL, Hoover S, Hrubes JD, Jones C, Joy M, Keisler R, Knox L, Lee AT, Leitch EM, Liu J, Lueker M, Luong-Van D, Mantz A, Marrone DP, McDonald M, McMahon JJ, Mehl J, Meyer SS, Mocanu L, Mohr JJ, Murray SS, Natoli T, Padin S, Plagge T, Pryke C, Rest A, Ruel J, Ruhl JE, Saliwanchik BR, Saro A, Sayre JT, Schaffer KK, Shaw L, Shirokoff E, Song J, Spieler HG, Staniszewski Z, Stark AA, Story K, Stubbs CW, Šuhada R, van Engelen A, Vanderlinde K, Vieira JD, Vikhlinin A, Williamson R, Zahn O and Zenteno A (2013), Feb. Galaxy Clusters Discovered via the Sunyaev-Zel'dovich Effect in the First 720 Square Degrees of the South Pole Telescope Survey. *Astrophys. J.* 763, 127. doi:10.1088/0004-637X/763/2/127. 1203.5775.
- Reichardt CL, Patil S, Ade PAR, Anderson AJ, Austermann JE, Avva JS, Baxter E, Beall JA, Bender AN, Benson BA, Bianchini F, Bleem LE, Carlstrom JE, Chang CL, Chaubal P, Chiang HC, Chou TL, Citron R, Corbett Moran C, Crawford TM, Crites AT, de Haan T, Dobbs MA, Everett W, Gallicchio J, George EM, Gilbert A, Gupta N, Halverson NW, Harrington N, Henning JW, Hilton GC, Holder GP, Holzapfel WL, Hrubes JD, Huang N, Hubmayr J, Irwin KD, Knox L, Lee AT, Li D, Lowitz A, Luong-Van D, McMahon JJ, Mehl J, Meyer SS, Millea M, Mocanu LM, Mohr JJ, Montgomery J, Nadolski A, Natoli T, Nibarger JP, Noble G, Novosad V, Omori Y, Padin S, Pryke C, Ruhl JE, Saliwanchik BR, Sayre JT, Schaffer KK, Shirokoff E, Sievers C, Smecher G, Spieler HG, Staniszewski Z, Stark AA, Tucker C, Vand erlinde K, Veach T, Vieira JD, Wang G, Whitehorn N, Williamson R, Wu WLK and Yefremenko V (2020), Feb. An Improved Measurement of the Secondary Cosmic Microwave Background Anisotropies from the SPT-SZ + SPTpol Surveys. *arXiv e-prints*, arXiv:2002.061972002.06197.
- Remazeilles M and Chluba J (2024), Oct. Evidence for relativistic Sunyaev-Zeldovich effect in Planck CMB maps with an average electron-gas temperature of  $T_e \approx 5$  keV. *arXiv e-prints*, arXiv:2410.02488doi:10.48550/arXiv.2410.02488. 2410.02488.
- Rephaeli Y (1995), May. Cosmic Microwave Background Comptonization by Hot Intraccluster Gas. *Astrophys. J.* 445: 33. doi:10.1086/175669.
- Robertson M and Lewis A (2024). How to detect lensing rotation. 2303.13313, <https://arxiv.org/abs/2303.13313>.
- Robertson NC and et al. (2021). Strong detection of the CMB lensing and galaxy weak lensing cross-correlation from ACT-DR4, Planck Legacy, and KiDS-1000. *Astron. Astrophys.* 649: A146. doi:10.1051/0004-6361/202039975. 2011.11613.
- Roy A, Lapi A, Spergel D and Baccigalupi C (2018), May. Observing patchy reionization with future CMB polarization experiments. *J. Cosmol. Astropart. Phys.* 2018 (5), 014. doi:10.1088/1475-7516/2018/05/014. 1801.02393.
- Roy A, van Engelen A, Gluscevic V and Battaglia N (2023), Jul. Probing the Circumgalactic Medium with Cosmic Microwave Background Polarization Statistical Anisotropy. *Astrophys. J.* 951 (1), 50. doi:10.3847/1538-4357/acd194. 2201.05076.
- Sachs RK and Wolfe AM (1967), Jan. Perturbations of a Cosmological Model and Angular Variations of the Microwave Background. *Astrophys. J.* 147: 73. doi:10.1086/148982.
- Salvati L, Douspis M and Aghanim N (2018), Jun. Constraints from thermal Sunyaev-Zel'dovich cluster counts and power spectrum combined with CMB. *Astron. Astrophys.* 614, A13. doi:10.1051/0004-6361/201731990. 1708.00697.
- Sayers J, Mroczkowski T, Zemcov M, Korngut PM, Bock J, Bulbul E, Czakon NG, Egami E, Golwala SR, Koch PM, Lin KY, Mantz A, Molnar SM, Moustakas L, Pierpaoli E, Rawle TD, Reese ED, Rex M, Shitanishi JA, Siegel S and Umetsu K (2013), Nov. A Measurement of the Kinetic Sunyaev-Zel'dovich Signal Toward MACS J0717.5+3745. *Astrophys. J.* 778 (1), 52. doi:10.1088/0004-637X/778/1/52. 1312.3680.
- Sazonov SY and Sunyaev RA (1999), Dec. Microwave polarization in the direction of galaxy clusters induced by the CMB quadrupole anisotropy. *Mon. Not. R. Astron. Soc.* 310 (3): 765–772. doi:10.1046/j.1365-8711.1999.02981.x. astro-ph/9903287.
- Schaan E and Ferraro S (2019), May. Foreground-immune cosmic microwave background lensing with shear-only reconstruction. *Physical Review Letters* 122 (18). ISSN 1079-7114. doi:10.1103/physrevlett.122.181301. <http://dx.doi.org/10.1103/PhysRevLett.122.181301>.
- Schaan E and et al. (ACTPol) (2016). Evidence for the kinematic Sunyaev-Zel'dovich effect with the Atacama Cosmology Telescope and velocity reconstruction from the Baryon Oscillation Spectroscopic Survey. *Phys. Rev. D* 93 (8): 082002. doi:10.1103/PhysRevD.93.082002. 1510.06442.
- Schaan E, Krause E, Eifler T, Doré O, Miyatake H, Rhodes J and Spergel DN (2017), Jun. Looking through the same lens: Shear calibration for LSST, Euclid, andWFIRST with stage 4 CMB lensing. *Phys. Rev. D* 95 (12), 123512. doi:10.1103/PhysRevD.95.123512. 1607.01761.
- Schaan E, Ferraro S, Amodeo S, Battaglia N, Aiola S, Austermann JE, Beall JA, Bean R, Becker DT, Bond RJ, Calabrese E, Calafut V, Choi SK, Denison EV, Devlin MJ, Duff SM, Duivenvoorden AJ, Dunkley J, Dünner R, Gallardo PA, Guan Y, Han D, Hill JC, Hilton GC, Hilton M, Hložek R, Hubmayr J, Huffenberger KM, Hughes JP, Koopman BJ, MacInnis A, McMahon J, Madhavacheril MS, Moodley K, Mroczkowski T, Naess S, Nati F, Newburgh LB, Niemack MD, Page LA, Partridge B, Salatino M, Sehgal N, Schillaci A, Sifón C, Smith KM, Spergel DN, Staggs S, Storer ER, Trac H, Ullom JN, Van Lanen J, Vale LR, van Engelen A, Magaña MV, Vavagiakis EM, Wollack EJ, Xu Z and Atacama Cosmology Telescope Collaboration (2021), Mar. Atacama Cosmology Telescope: Combined kinematic and thermal Sunyaev-Zel'dovich measurements from BOSS CMASS and LOWZ halos. *Phys. Rev. D* 103 (6), 063513. doi:10.1103/PhysRevD.103.063513. 2009.05557.
- Schiappucci E, Bianchini F, Aguena M, Archipley M, Balkenhol L, Bleem LE, Chaubal P, Crawford TM, Grandis S, Omori Y, Reichardt CL, Rozo E, Rykoff ES, To C, Abbott TMC, Ade PAR, Alves O, Anderson AJ, Andrade-Oliveira F, Annis J, Avva JS, Bacon D, Benabed K, Bender AN, Benson BA, Bernstein GM, Bertin E, Bocquet S, Bouchet FR, Brooks D, Burke DL, Carlstrom JE, Carnero Rosell A, Carrasco Kind M, Carretero J, Cecil TW, Chang CL, Chichura PM, Chou TL, Costanzi M, Cukierman A, da Costa LN, Daley C, de Haan T, Desai S, Dibert KR, Diehl HT, Dobbs MA, Doel P, Doux C, Dutcher D, Everett S, Everett W, Feng C, Ferguson KR, Ferrero I, Ferté A, Flaugher B, Foster A, Frieman J, Galli S, Gamberale AE, García-Bellido J, Gardner RW, Gatti M, Giannantonio T, Goeckner-Wald N, Gruen D, Gualtieri R, Guns S, Gutierrez G, Halverson NW, Hinton SR, Hirven E, Holder GP, Hollowood DL, Holzapfel WL, Honscheid K, Hood JC, Huang N, James DJ, Knox L, Korman M, Kuehn K, Kuo CL, Lahav O, Lee AT, Lidman C, Lima M, Lowitz AE, Lu C, March M, Mena-Fernández J, Menanteau F, Millea M, Miquel R, Mohr JJ, Montgomery J, Muir J, Natoli T, Noble GI, Novosad V, Ogando RLC, Padin S, Pan Z, Paz-Chinchón F, Pereira MES, Pieries A, Plazas Malagón AA, Prabhu K, Prat J, Quan W, Rahlin A, Raveri M, Rodriguez-Monroy M, Romer AK, Rouble M, Ruhl JE, Sanchez E, Scarpine V, Schubnell M, Smecher G, Smith M, Soares-Santos M, Sobrin JA, Suchyta E, Suzuki A, Tarle G, Thomas D, Thompson KL,

- Thorne B, Tucker C, Umita C, Vieira JD, Vincenzi M, Wang G, Weaverdyck N, Weller J, Whitehorn N, Wu WLK, Yefremenko V, Young MR, SPT-3G and DES Collaborations (2023), Feb. Measurement of the mean central optical depth of galaxy clusters via the pairwise kinematic Sunyaev-Zel'dovich effect with SPT-3G and DES. *Phys. Rev. D* 107 (4), 042004. doi:10.1103/PhysRevD.107.042004. 2207.11937.
- Schutt T, Maniyar AS, Schaan E, Coulton WR and Mishra N (2024), May. New temperature inversion estimator to detect CMB patchy screening by large-scale structure. *Phys. Rev. D* 109 (10), 103539. doi:10.1103/PhysRevD.109.103539. 2401.13040.
- Seljak U (1996), May. Gravitational Lensing Effect on Cosmic Microwave Background Anisotropies: A Power Spectrum Approach. *Astrophys. J.* 463: 1–+. doi:10.1086/177218. arXiv:astro-ph/9505109.
- Sgier R, Lorenz C, Refregier A, Fluri J, Zürcher D and Tarsitano F (2021), 10. Combined 13 × 2-point analysis of the Cosmic Microwave Background and Large-Scale Structure: implications for the  $S_8$ -tension and neutrino mass constraints 2110.03815.
- Shaw LD, Rudd DH and Nagai D (2012), Sep. Deconstructing the Kinetic SZ Power Spectrum. *Astrophys. J.* 756, 15. doi:10.1088/0004-637X/756/1/15. 1109.0553.
- Shen D, Schaan E and Ferraro S (2024), Aug. Cmb lensing power spectrum without noise bias. *Physical Review D* 110 (4). ISSN 2470-0029. doi:10.1103/physrevd.110.043523. <http://dx.doi.org/10.1103/PhysRevD.110.043523>.
- Sherwin BD, Das S, Hajian A, Addison G, Bond JR, Crichton D, Devlin MJ, Dunkley J, Gralla MB, Halpern M, Hill JC, Hincks AD, Hughes JP, Huffenberger K, Hlozek R, Kosowsky A, Louis T, Marriage TA, Marsden D, Menanteau F, Moodley K, Niemack MD, Page LA, Reese ED, Sehgal N, Sievers J, Sifón C, Spergel DN, Staggs ST, Switzer ER and Wollack E (2012), Oct. The Atacama Cosmology Telescope: Cross-correlation of cosmic microwave background lensing and quasars. *Phys. Rev. D* 86 (8), 083006. doi:10.1103/PhysRevD.86.083006. 1207.4543.
- Sherwin BD, van Engelen A, Sehgal N, Madhavacheril M, Addison GE, Aiola S, Allison R, Battaglia N, Becker DT, Beall JA, Bond JR, Calabrese E, Datta R, Devlin MJ, Dünner R, Dunkley J, Fox AE, Gallardo P, Halpern M, Hasselfeld M, Henderson S, Hill JC, Hilton GC, Hubmayr J, Hughes JP, Hincks AD, Hlozek R, Huffenberger KM, Koopman B, Kosowsky A, Louis T, Maurin L, McMahon J, Moodley K, Naess S, Nati F, Newburgh L, Niemack MD, Page LA, Sievers J, Spergel DN, Staggs ST, Thornton RJ, Van Lanen J, Vavagiakis E and Wollack EJ (2017), Jun. Two-season Atacama Cosmology Telescope polarimeter lensing power spectrum. *Phys. Rev. D* 95 (12), 123529. doi:10.1103/PhysRevD.95.123529. 1611.09753.
- Silk J (1967), Sep. Fluctuations in the Primordial Fireball. *Nature* 215 (5106): 1155–1156. doi:10.1038/2151155a0.
- Singh S, Mandelbaum R and Brownstein JR (2017), Cross-correlating Planck CMB lensing with SDSS: Lensing-lensing and galaxy-lensing cross-correlations. *Mon. Not. Roy. Astron. Soc.* 464 (2): 2120–2138. doi:10.1093/mnras/stw2482. 1606.08841.
- Smith KM and Ferraro S (2017), Jul. Detecting Patchy Reionization in the Cosmic Microwave Background. *Physical Review Letters* 119 (2), 021301. doi:10.1103/PhysRevLett.119.021301.
- Smith KM, Zahn O and Dore O (2007), Detection of Gravitational Lensing in the Cosmic Microwave Background. *Phys. Rev. D* 76: 043510. doi:10.1103/PhysRevD.76.043510. 0705.3980.
- Smith KM, Madhavacheril MS, Münchmeyer M, Ferraro S, Giri U and Johnson MC (2018), Oct. KSZ tomography and the bispectrum. *arXiv e-prints*, arXiv:1810.13423doi:10.48550/arXiv.1810.13423. 1810.13423.
- Sobrin JA, Anderson AJ, Bender AN, Benson BA, Dutcher D, Foster A, Goeckner-Wald N, Montgomery J, Nadolski A, Rahlin A, Ade PAR, Ahmed Z, Anderes E, Archipley M, Austermann JE, Avva JS, Aylor K, Balkenhol L, Barry PS, Thakur RB, Benabed K, Bianchini F, Bleem LE, Bouchet FR, Bryant L, Byrum K, Carlstrom JE, Carter FW, Cecil TW, Chang CL, Chaubal P, Chen G, Cho HM, Chou TL, Cliche JF, Crawford TM, Cukierman A, Daley C, Haan TD, Denison EV, Dibert K, Ding J, Dobbs MA, Everett W, Feng C, Ferguson KR, Fu J, Galli S, Gambrel AE, Gardner RW, Gualtieri R, Guns S, Gupta N, Guyser R, Halverson NW, Harke-Hosemann AH, Harrington NL, Henning JW, Hilton GC, Hivon E, Holder GP, Holzapfel WL, Hood JC, Howe D, Huang N, Irwin KD, Jeong OB, Jonas M, Jones A, Khaire TS, Knox L, Kofman AM, Korman M, Kubik DL, Kuhlmann S, Kuo CL, Lee AT, Leitch EM, Lowitz AE, Lu C, Meyer SS, Michalik D, Millea M, Natoli T, Nguyen H, Noble GI, Novosad V, Omori Y, Padin S, Pan Z, Paschos P, Pearson J, Posada CM, Prabhu K, Quan W, Reichardt CL, Riebel D, Riedel B, Rouble M, Ruhl JE, Saliwanchik B, Sayre JT, Schiappucci E, Shirokoff E, Smecher G, Stark AA, Stephen J, Story KT, Suzuki A, Tandoi C, Thompson KL, Thorne B, Tucker C, Umita C, Vale LR, Vanderlinde K, Vieira JD, Wang G, Whitehorn N, Wu WLK, Yefremenko V, Yoon KW and Young MR (2022), Feb. The Design and Integrated Performance of SPT-3G. *Astrophys. J. Suppl. Ser.* 258 (2), 42. doi:10.3847/1538-4365/ac374f. 2106.11202.
- Soergel B, Flender S, Story KT, Bleem L, Giannantonio T, Efstatios G, Rykoff E, Benson BA, Crawford T, Dodelson S, Habib S, Heitmann K, Holder G, Jain B, Rozo E, Saro A, Weller J, Abdalla FB, Allam S, Annis J, Armstrong R, Benoit-Lévy A, Bernstein GM, Carlstrom JE, Carnero Rosell A, Carrasco Kind M, Castander FJ, Chiu I, Chown R, Croce M, Cunha CE, D'Andrea CB, da Costa LN, de Haan T, Desai S, Diehl HT, Dietrich JP, Doel P, Estrada J, Evrard AE, Flaugher B, Fosalba P, Frieman J, Gaztanaga E, Gruen D, Gruendl RA, Holzapfel WL, Honscheid K, James DJ, Keisler R, Kuehn K, Kuropatkin N, Lahav O, Lima M, Marshall JL, McDonald M, Melchior P, Miller CJ, Miquel R, Nord B, Ogando R, Omori Y, Plazas AA, Rapetti D, Reichardt CL, Romer AK, Roodman A, Saliwanchik BR, Sanchez E, Schubnell M, Sevilla-Noarbe I, Sheldon E, Smith RC, Soares-Santos M, Sobreira F, Stark A, Suchyta E, Swanson MEC, Tarle G, Thomas D, Vieira JD, Walker AR, Whitehorn N, DES Collaboration and SPT Collaboration (2016), Sep. Detection of the kinematic Sunyaev-Zel'dovich effect with DES Year 1 and SPT. *Mon. Not. R. Astron. Soc.* 461: 3172–3193. doi:10.1093/mnras/stw1455. 1603.03904.
- Staniszewski Z, Ade PAR, Aird KA, Benson BA, Bleem LE, Carlstrom JE, Chang CL, Cho HM, Crawford TM, Crites AT, de Haan T, Dobbs MA, Halverson NW, Holder GP, Holzapfel WL, Hrbres JD, Joy M, Keisler R, Lanting TM, Lee AT, Leitch EM, Loehr A, Lueker M, McMahon JJ, Mehl J, Meyer SS, Mohr JJ, Montroy TE, Ngeow CC, Padin S, Plagge T, Pryke C, Reichardt CL, Ruhl JE, Schaffer KK, Shaw L, Shirokoff E, Spieler HG, Stalder B, Stark AA, Vanderlinde K, Vieira JD, Zahn O and Zenteno A (2009), Jul. Galaxy clusters discovered with a sunyaev-zel'dovich effect survey. *The Astrophysical Journal* 701 (1): 32–41. ISSN 1538-4357. doi:10.1088/0004-637x/701/1/32. <http://dx.doi.org/10.1088/0004-637x/701/1/32>.
- Stebbins A (2006), Measuring velocities using the CMB & LSS. *New Astron. Rev.* 50: 918–924. doi:10.1016/j.newar.2006.09.028.
- Stein G, Alvarez MA, Bond JR, Engelen AV and Battaglia N (2020), Oct. The websky extragalactic cmb simulations. *Journal of Cosmology and Astroparticle Physics* 2020 (10): 012–012. ISSN 1475-7516. doi:10.1088/1475-7516/2020/10/012. <http://dx.doi.org/10.1088/1475-7516/2020/10/012>.
- Stompor R and Efstatios G (1999), Feb. Gravitational lensing of cosmic microwave background anisotropies and cosmological parameter estimation. *Monthly Notices of the Royal Astronomical Society* 302 (4): 735–747. ISSN 1365-2966. doi:10.1046/j.1365-8711.1999.02174.x. <http://dx.doi.org/10.1046/j.1365-8711.1999.02174.x>.
- Story KT, Hanson D, Ade PAR, Aird KA, Austermann JE, Beall JA, Bender AN, Benson BA, Bleem LE, Carlstrom JE, Chang CL, Chiang HC, Cho HM, Citron R, Crawford TM, Crites AT, Haan TD, Dobbs MA, Everett W, Gallicchio J, Gao J, George EM, Gilbert A, Halverson NW, Harrington N, Henning JW, Hilton GC, Holder GP, Holzapfel WL, Hoover S, Hou Z, Hrbres JD, Huang N, Hubmayr J, Irwin KD, Keisler R, Knox L, Lee AT, Leitch EM, Li D, Liang C, Luong-Van D, McMahon JJ, Mehl J, Meyer SS, Mocanu L, Montroy TE, Natoli T, Nibarger JP, Novosad V, Padin S, Pryke C, Reichardt CL, Ruhl JE, Saliwanchik BR, Sayre JT, Schaffer KK, Smecher G, Stark AA, Tucker C, Vanderlinde K, Vieira JD, Wang G, Whitehorn N, Yefremenko V and Zahn O (2015), Aug. A measurement of the cosmic microwave background gravitational lensing potential from 100 square degrees of sptpol data. *The Astrophysical Journal* 810 (1): 50. ISSN 1538-4357. doi:10.1088/0004-637x/810/1/50. <http://dx.doi.org/10.1088/0004-637x/810/1/50>.

- Sunyaev RA and Zeldovich YB (1970), Mar. The Spectrum of Primordial Radiation, its Distortions and their Significance. *Comments on Astrophysics and Space Physics* 2: 66.
- Sunyaev RA and Zeldovich YB (1972), Nov. The Observations of Relic Radiation as a Test of the Nature of X-Ray Radiation from the Clusters of Galaxies. *Comments on Astrophysics and Space Physics* 4: 173.
- Sunyaev RA and Zeldovich YB (1980), Feb. The velocity of clusters of galaxies relative to the microwave background - The possibility of its measurement. *Mon. Not. R. Astron. Soc.* 190: 413–420. doi:10.1093/mnras/190.3.413.
- Swetz DS, Ade PAR, Amiri M, Appel JW, Battistelli ES, Burger B, Chervenak J, Devlin MJ, Dicker SR, Dorries WB, Dünner R, Essinger-Hileman T, Fisher RP, Fowler JW, Halpern M, Hasselfield M, Hilton GC, Hincks AD, Irwin KD, Jarosik N, Kaul M, Klein J, Lau JM, Limon M, Marriage TA, Marsden D, Martocci K, Mauskopf P, Moseley H, Netterfield CB, Niemack MD, Nolta MR, Page LA, Parker L, Staggs ST, Stryzak O, Switzer ER, Thornton R, Tucker C, Wollack E and Zhao Y (2011), Jun. Overview of the Atacama Cosmology Telescope: Receiver, Instrumentation, and Telescope Systems. *Astrophys. J. Suppl. Ser.* 194, 41. doi:10.1088/0067-0049/194/2/41. 1007.0290.
- Todarello E, Regis M, Bianchini F, Singal J, Branchini E, Cowie FJ, Heston S, Horiuchi S, Lucero D and Offringa A (2024), May. Constraints on the origin of the radio synchrotron background via angular correlations. *Mon. Not. R. Astron. Soc.* 530 (3): 2994–3004. doi:10.1093/mnras/stae876. 2311.17641.
- Tului R and Laguna P (1995), Jun. The Imprint of Proper Motion of Nonlinear Structures on the Cosmic Microwave Background. *Astrophys. J. Lett.* 445: L73. doi:10.1086/187893. astro-ph/9501059.
- van Engelen A, Keister R, Zahn O, Aird KA, Benson BA, Bleem LE, Carlstrom JE, Chang CL, Cho HM, Crawford TM, Crites AT, de Haan T, Dobbs MA, Dudley J, George EM, Halverson NW, Holder GP, Holzapfel WL, Hoover S, Hou Z, Hrubes JD, Joy M, Knox L, Lee AT, Leitch EM, Lueker M, Luong-Van D, McMahon JJ, Mehl J, Meyer SS, Millea M, Mohr JJ, Montroy TE, Natoli T, Padin S, Plagge T, Pryke C, Reichardt CL, Ruhl JE, Sayre JT, Schaffer KK, Shaw L, Shirokoff E, Spieler HG, Staniszewski Z, Stark AA, Story K, Vanderlinde K, Vieira JD and Williamson R (2012), Aug. A measurement of gravitational lensing of the microwave background using south pole telescope data. *The Astrophysical Journal* 756 (2): 142. ISSN 1538-4357. doi:10.1088/0004-637X/756/2/142. http://dx.doi.org/10.1088/0004-637X/756/2/142.
- van Engelen A and et al. (ACT) (2015). The Atacama Cosmology Telescope: Lensing of CMB Temperature and Polarization Derived from Cosmic Infrared Background Cross-Correlation. *Astrophys. J.* 808 (1): 7. doi:10.1088/0004-637X/808/1/7. 1412.0626.
- Wright EL (1979), Sep. Distortion of the microwave background by a hot intergalactic medium. *Astrophys. J.* 232: 348–351. doi:10.1086/157294.
- Wu WLK, Mocanu LM, Ade PAR, Anderson AJ, Austermann JE, Avva JS, Beall JA, Bender AN, Benson BA, Bianchini F, Bleem LE, Carlstrom JE, Chang CL, Chiang HC, Citron R, Corbett Moran C, Crawford TM, Crites AT, de Haan T, Dobbs MA, Everett W, Gallicchio J, George EM, Gilbert A, Gupta N, Halverson NW, Harrington N, Henning JW, Hilton GC, Holder GP, Holzapfel WL, Hou Z, Hrubes JD, Huang N, Hubmayr J, Irwin KD, Knox L, Lee AT, Li D, Lowitz A, Manzotti A, McMahon JJ, Meyer SS, Millea M, Montgomery J, Nadolski A, Natoli T, Nibarger JP, Noble GI, Novosad V, Omori Y, Padin S, Patil S, Pryke C, Reichardt CL, Ruhl JE, Salwanchik BR, Sayre JT, Schaffer KK, Sievers C, Simard G, Smecher G, Stark AA, Story KT, Tucker C, Vanderlinde K, Veach T, Vieira JD, Wang G, Whitehorn N and Yefremenko V (2019), Oct. A Measurement of the Cosmic Microwave Background Lensing Potential and Power Spectrum from 500 deg<sup>2</sup> of SPTpol Temperature and Polarization Data. *Astrophys. J.* 884 (1), 70. doi:10.3847/1538-4357/ab4186. 1905.05777.
- Yasini S, Mirzatuny N and Pierpaoli E (2019). Pairwise Transverse Velocity Measurement with the Rees–Sciama Effect. *Astrophys. J. Lett.* 873 (2): L23. doi:10.3847/2041-8213/ab0bfe. 1812.04241.
- Zaldarriaga M (2000). Lensing of the CMB: Non-Gaussian aspects. *Phys. Rev. D* 62: 063510. doi:10.1103/PhysRevD.62.063510. astro-ph/9910498.
- Zaldarriaga M and Seljak U (1998), Jul. Gravitational lensing effect on cosmic microwave background polarization. *Phys. Rev. D* 58 (2), 023003. doi:10.1103/PhysRevD.58.023003. astro-ph/9803150.
- Zubeldia I and Challinor A (2019), Apr. Cosmological constraints from Planck galaxy clusters with CMB lensing mass bias calibration. *arXiv e-prints*, arXiv:1904.07887 1904.07887.